Local-density approach and quasiparticle levels for generalized Hubbard Hamiltonians

P. Pou, R. Pérez, F. Flores, A. Levy Yeyati, A. Martin-Rodero, J. M. Blanco, F. J. García-Vidal, and J. Ortega
Departamento de Física Teórica de la Materia Condensada (C-V), Facultad de Ciencias, Universidad Autónoma de Madrid, E-28049 Madrid, Spain

(Received 29 November 1999)

This paper presents a general method to describe and analyze electron correlation effects in local-orbital electronic structure calculations using a generalized Hubbard Hamiltonian. In our approach, we first introduce a local density formalism where the total energy of the system is obtained as a function of the orbital occupancies $\{n_i\}$ associated with each local orbital; in particular, exchange and correlation local potentials are presented for a multilevel case. In parallel, using the dynamical mean field approximation, a many-body solution is obtained by means of a local self-energy that appropriately interpolates between the low and high correlation limits. We also show that the local density and the many-body solutions are linked through charge consistency conditions. These two solutions are applied to a multilevel Anderson impurity and to a multiband Hubbard lattice, our results showing the high accuracy of the approach presented in this paper. Further on, we discuss how to apply our previous analysis to the case of crystals and molecules and analyze several examples: bulk Si, and HF and H_2O molecules. The good results obtained for these cases show that our approach for the description of correlation effects offers an interesting alternative to the well-established density functional methods based on the calculation of the electron density $\rho(\vec{r})$.

I. INTRODUCTION

The prediction of the electronic and geometric structure of a solid requires the calculation of the quantum-mechanical properties of a system of interacting electrons in the presence of a given configuration of nuclei. Different approaches have been developed over the years to handle this complicated many-body problem. Density functional theory (DFT) (Refs. 1–3) provides an exact mapping of the problem of a strongly interacting electron system (in the presence of the nuclei) onto that of a single particle moving in an effective potential due to all the other electrons. With this approach, properties such as the total energy of the system could be calculated exactly. However, the effective potential—in particular, the so called exchange-correlation potential—is not known exactly and further approximations are needed. The local density approximation[4] (LDA) assumes that the exchange-correlation functional is purely local and can be calculated as a function of the local charge density. This approach provides accurate total energy differences between related structures but total cohesive energies can be in error by more than 20%.[5] The generalized gradient approximation[6] (GGA), where both the charge density and its gradient are used to calculate the exchange-correlation functional, improves the LDA results but does not fix completely the problem with the cohesive energies. Although total energy calculations can be performed quite accurately with these approximations, neither of them provides the correct quasiparticle spectrum of the system.[5] A new approach based on an energy-dependent nonlocal functional is necessary for this purpose, and further approximations are needed to make the problem tractable. The GW approximation[7–10] has been applied to metals and semiconductors and provides an energy spectrum in good agreement with the experiment. We also mention the LDA+U method[11] which offers a very simple way of correcting for the main deficiency of the local density approximation as far as band gaps are concerned.

All these methods have been traditionally implemented using a plane wave basis for the expansion of the electronic wave functions.[12] Recently, different methods based on local orbital basis have been developed.[13–22] Local orbital basis sets may be used to improve significantly the computational performance of electronic structure calculations. For example, efficient first-principles tight-binding molecular dynamics methods can be devised using appropriate atomiclike basis sets, and order-*N* algorithms can be easily implemented in a local orbital framework.[23]

On the other hand, local orbital schemes are the natural playground for the models, such as the Anderson or Hubbard Hamiltonians, which have been used to describe systems where correlation effects are so important that the band picture, implicit in all the approaches described above, breaks down. The established methods in this field are based on Green's functions and self-energies which are naturally written in terms of local orbitals. This reflects the fact that the more important contributions to the correlation energy come from the local intrasite terms. The idea of locality even pervades the formulation of new approaches. The dynamic mean field method[24] (DMF) is a new approach which has been developed over recent years and has led to some progress in our understanding of these correlated systems. The essential idea is to replace a lattice model by a single site impurity problem embedded in an effective medium determined self-consistently. In this way, only local quantum fluctuations are included in the calculation.

Traditionally these two fields, electronic structure calculations based on LDA or GGA and PW basis for realistic materials, and sophisticated many body techniques applied to model Hamiltonians appear as two completely different, even opposite, approaches to the electronic properties of the system. However, once the electronic structure calculations are formulated in terms of local orbitals several connections

between the two approaches emerge naturally.

The purpose of this paper is to present a *general approach* to describe and analyze electron correlation effects in local-orbital electronic structure calculations. This new approach also provides a connection between simple models (e.g., the Hubbard model), more sophisticated models (e.g., the generalized Hubbard model), and fully first-principles total energy methods. Therefore, the discussion presented below is also useful for deriving the parameters appearing in the simple models from first-principles calculations.[25]

The main two points discussed in this paper are as follows.

(i) How the contributions due to the correlation energy can be included in a local density (LD) first-principles total energy method. In this approach, the correlation energy is obtained as an explicit function of the orbital occupancies $\{n_i\}$ in contrast with standard density functional approaches such as the LDA or GGA.

(ii) How to obtain the quasiparticle spectrum going beyond the LD solution.

The generalized Hubbard Hamiltonian

$$\hat{H}=\hat{H}^{\mathrm{OE}}+\hat{H}^{\mathrm{MB}}, \tag{1}$$

where $\hat{H}^{\mathrm{OE}}$ defines the one-electron contribution

$$\hat{H}^{\mathrm{OE}}=\sum_{i\alpha,\sigma} E^{\sigma}_{i\alpha}\hat{n}_{i\alpha,\sigma}+\sum_{i\alpha\neq j\beta,\sigma} t^{\sigma}_{i\alpha,j\beta}\hat{c}^{\dagger}_{i\alpha,\sigma}\hat{c}_{j\beta,\sigma} \tag{2}$$

and $\hat{H}^{\mathrm{MB}}$ the many-body term

$$\hat{H}^{\mathrm{MB}}=\frac{1}{2}\sum_{i,\alpha\sigma\neq\beta\sigma'} U_i\hat{n}_{i\alpha,\sigma}\hat{n}_{i\beta,\sigma'} + \frac{1}{2}\sum_{i\neq j}^{\alpha\sigma,\beta\sigma'} J_{i\alpha,j\beta}\hat{n}_{i\alpha,\sigma}\hat{n}_{j\beta,\sigma'}, \tag{3}$$

plays a central role in the discussion presented below. In Eqs. (2) and (3), $\hat{c}^{\dagger}$, $\hat{c}$, and $\hat{n}$ are the usual creation, annihilation, and number operators, respectively. In this paper we will discuss in detail how the correlation energy and quasiparticle spectrum for this Hamiltonian can be obtained. We stress here that Hamiltonian (1) includes most of the many-body effects appearing in linear combination of atomic orbital (LCAO) Hamiltonians. In Sec. II, we discuss our general local density formalism for generalized Hubbard Hamiltonians and analyze the Hartree, exchange, and extra-atomic correlation potentials for each localized orbital. In Sec. II it is also shown how, by using a dynamical mean field (DMF) approximation, the generalized Hubbard Hamiltonian can be mapped onto a ''reduced'' Hubbard Hamiltonian

$$\hat{H}^{r}=\sum_{i\alpha\sigma}\tilde{E}^{\sigma}_{i\alpha}\hat{n}_{i\alpha\sigma}+\sum_{i\alpha\neq j\beta,\sigma} t^{\sigma}_{i\alpha,j\beta}\hat{c}^{\dagger}_{i\alpha\sigma}\hat{c}_{j\beta\sigma} + \frac{1}{2}\sum_{i,\alpha\sigma\neq\beta\sigma'}\tilde{U}_i\hat{n}_{i\alpha\sigma}\hat{n}_{i\beta\sigma'},$$

where $\tilde{E}^{\sigma}_{i\alpha}$ is a renormalized $i\alpha$ level and $\tilde{U}_i$ an effective intrasite Coulomb interaction. This reduced Hubbard Hamiltonian is then analyzed (Sec. III) by means of many-body techniques (Green functions, self-energies), in two limits $\tilde{U}/t\rightarrow 0$ and $\tilde{U}/t\rightarrow\infty$. From this analysis, general expressions for the intra-atomic correlation energy and the self-energy are proposed, using an interpolation between the above two limits. As discussed in Sec. III, these results can be used to analyze the generalized Hubbard Hamiltonian following two alternative procedures: (a) many-body and (b) LD solutions. These cases are shown to be linked through the charge self-consistent conditions. The expression obtained in this section for the intra-atomic correlation energy will be used in Sec. V as one of the main contributions to the exchange-correlation energy in our first-principles LD total-energy method for crystals and molecules.

The ideas introduced in Sec. III are applied to a multilevel Anderson model and to a Hubbard lattice in Sec. IV. The results discussed in this section for highly correlated systems show the accuracy and quality of the approximations introduced in this paper.

In Sec. V, we discuss how to apply our previous analysis to the case of crystals or molecules. The case of crystals allows us to make contact with conventional DFT calculations, while the case of small molecules shows how to go beyond the DMF approximation. In this section we show how the results obtained in Secs. II and III for the exchange-correlation energy corresponding to the generalized Hubbard Hamiltonian can be extended and applied to LD first-principles total energy calculations. In particular, the results obtained by using this method show that the approach presented in this paper for the description of correlation effects offers an interesting alternative to the well-established density functional methods based on the electron density $\rho(\vec{r})$ (LDA,GGA).

Finally, we mention that, regarding the LD-LCAO approach, this paper is a continuation of Ref. 26, where the basic ideas were first introduced. In this work, we consider the possibility of having degenerate atomic orbitals and present, for this more general case, the many-body orbital potentials necessary for performing a fully consistent local density-LCAO calculation. For the sake of completeness we discuss briefly, however, in Sec. II the main ideas already presented in Ref. 26.

II. LOCAL DENSITY FORMALISM FOR GENERALIZED HUBBARD HAMILTONIANS

In this paper, we take as our starting point Hamiltonian (1). Notice that in Eq. (3), U_i represents the intratomic interaction between orbitals $i\alpha\sigma$ and $i\beta\sigma'$ located in the same site i and $J_{i\alpha,j\beta}$ defines the interatomic Coulomb interaction between orbitals α and β in different sites i and j. In this paper we assume the intratomic Coulomb interaction U_i to be the same for all the i orbitals; this implies neglecting effects associated with Hund's rules as is commonly done in the generalized Hubbard Hamiltonian (a more general analysis including Hund's rules and following the discussion presented in this paper will be published elsewhere). In Eq. (2), E and t describe the different atomic levels and their hopping interactions. We also assume that any intratomic hopping interaction is zero; this restriction will be removed in Sec. V.

Hamiltonian (1) has been used as the basic approach to analyze many different correlation problems. The restricted

Hubbard Hamiltonian is obtained by taking $J_{i\alpha,j\beta}=0$ in Hamiltonian (3): we shall discuss below how, upon given conditions, this restricted Hamiltonian with renormalized parameters plays an important role for defining intratomic correlation effects.

A. Local density equations

Following the LD approach introduced in Ref. 26, the total energy of the system described by Hamiltonian (1) can be shown to be a *function* of the orbital occupation numbers $n_{i\alpha\sigma}=\langle\hat{n}_{i\alpha\sigma}\rangle$ where $\langle\rangle$ indicate the expectation value in the ground state:

$$E=E[n_{1\uparrow},n_{1\downarrow},n_{2\uparrow},n_{2\downarrow},n_{i\alpha\sigma}\cdots]=E[\{n_{i\alpha\sigma}\}]. \tag{4}$$

In similarity with standard DF theory, the ground-state orbital occupation numbers are the set $n_{i\alpha\sigma}$ that minimizes $E[\{n_{i\alpha\sigma}\}]$; this minimization process is equivalent to the self-consistent solution of an effective one-electron Hamiltonian $\hat{H}^{\rm eff}$, which depends itself on these occupation numbers. In what follows, we show how $\hat{H}^{\rm eff}$ can be defined in terms of the parameters of Hamiltonian (1) and the orbital occupation numbers.

It is useful to split the total energy in Eq. (4) into the one-electron T and many-body $E^{\rm MB}$ contributions

$$E[\{n_{i\alpha\sigma}\}]=T[\{n_{i\alpha\sigma}\}]+E^{\rm MB}[\{n_{i\alpha\sigma}\}], \tag{5}$$

where T is the mean value of $\hat{H}^{\rm OE}$ for the ground state of $\hat{H}^{\rm eff}$ [Eq. (6) below]; then, following Kohn and Sham, we can introduce the following effective Hamiltonian:

$$\hat{H}^{\rm eff}=\sum_{i\alpha,\sigma}(E^{\sigma}_{i\alpha}+V^{\rm MB}_{i\alpha,\sigma})\hat{n}_{i\alpha,\sigma}+\sum_{\sigma,(i\alpha,j\beta)}t^{\sigma}_{i\alpha,j\beta}(\hat{c}^{\dagger}_{i\alpha,\sigma}\hat{c}_{j\beta,\sigma}+\hat{c}^{\dagger}_{j\beta,\sigma}\hat{c}_{i\alpha,\sigma}), \tag{6}$$

where

$$V^{\rm MB}_{i\alpha,\sigma}=\frac{\partial E^{\rm MB}[\{n_{i\alpha\sigma}\}]}{\partial n_{i\alpha,\sigma}}. \tag{7}$$

Solving Eqs. (6), (7) self-consistently we can calculate the set $\{n_{i\alpha\sigma}\}$ for the ground state, and using Eq. (5) we obtain the total energy of the system.

B. Hartree and exchange energies

Obviously, the main problem in this approach is to determine $E^{\rm MB}$ in Eq. (5), as a function of the occupation numbers. Again, it is convenient to split this term into the so-called Hartree, exchange, and correlation contributions. While it is straightforward to write down the functional dependence of the Hartree term, exchange and correlation contributions are more involved. The following discussion describes the procedure to calculate $E^{X}[\{n_{i\alpha\sigma}\}]$ and $E^{C}[\{n_{i\alpha\sigma}\}]$.

From Eq. (1), we see that the Hartree contribution is given by

$$E^{H}[\{n_{i\alpha\sigma}\}]=\frac{1}{2}\sum_{i,\alpha\sigma\neq\beta\sigma'}U_i n_{i\alpha\sigma}n_{i\beta\sigma'}+\frac{1}{2}\sum_{i\neq j}^{\alpha\sigma,\beta\sigma'}J_{i\alpha,j\beta}n_{i\alpha\sigma}n_{j\beta\sigma'} \tag{8}$$

while the exchange energy is

$$E^{X}[\{n_{i\alpha\sigma}\}]=-\frac{1}{2}\sum_{i\neq j}^{\alpha,\beta,\sigma}J_{i\alpha,j\beta}n_{i\alpha\sigma;j\beta\sigma}n_{j\beta\sigma;i\alpha\sigma} \tag{9}$$

with $n_{i\alpha\sigma;j\beta\sigma}=\langle\hat{c}^{\dagger}_{i\alpha\sigma}\hat{c}_{j\beta\sigma}\rangle$. Now, we follow the argument given in Ref. 26, and make use of the sum rule

$$\sum_{j\beta\neq i\alpha}n_{i\alpha\sigma;j\beta\sigma}n_{j\beta\sigma;i\alpha\sigma}=n_{i\alpha\sigma}(1-n_{i\alpha\sigma}) \tag{10}$$

to write

$$E^{X}[\{n_{i\alpha\sigma}\}]=-\frac{1}{2}\sum_{i\alpha\sigma}J_{i\alpha\sigma}n_{i\alpha\sigma}(1-n_{i\alpha\sigma}) \tag{11}$$

which yields the exchange energy as the interaction $J_{i\alpha\sigma}$ [see Eq. (15) below], between the charge $n_{i\alpha\sigma}$ and its hole $(1-n_{i\alpha\sigma})$. The extra $n_{i\alpha\sigma}$ hole needed for a total exchange hole of 1 is associated with the self-interaction correction that is automatically included in our formalism.

At this point it is convenient to comment that the exchange pair correlation function $g_{\sigma}(i\alpha,j\beta)$ is defined[26] by the equation

$$n_{i\alpha\sigma;j\beta\sigma}n_{j\beta\sigma;i\alpha\sigma}=n_{i\alpha\sigma}g_{\sigma}(i\alpha,j\beta) \tag{12}$$

and

$$\sum_{j\beta\neq i\alpha}g_{\sigma}(i\alpha,j\beta)=1-n_{i\alpha\sigma}. \tag{13}$$

In our discussion, we assume to have in the initial Hamiltonian (1), $t_{i\alpha,i\beta}=0$, and a symmetry around each lattice site such that

$$n_{i\alpha\sigma;i\beta\sigma}=0. \tag{14}$$

This basically means that the exchange hole around the orbital $i\alpha$ is extended beyond the local site i. This allows us to write the effective interaction $J_{i\alpha\sigma}$ [see Eq. (11)] as follows:

$$J_{i\alpha\sigma}=X(n_{i\alpha\sigma})J^{\rm NN}_{i\alpha}, \tag{15}$$

where $J^{\rm NN}_{i\alpha}$ is the mean Coulomb interaction between an electron in the $i\alpha\sigma$ orbital and another electron in the nearest-neighbor sites, and $X(n_{i\alpha\sigma})$ a parameter, smaller than 1, measuring how the exchange hole associated with the $i\alpha\sigma$ orbital extends around the i site. In Ref. 26 we have shown that, for a three-dimensional crystal, $X(n_{i\alpha\sigma})$ is practically constant in the occupancy range $0.15<n_{i\alpha\sigma}<0.85$, with values between 0.7 and 0.8 for metals; in semiconductors, we have found, however, that $X(n_{i\alpha\sigma})$ is around 0.90–0.95 for the same range of occupancies. In both cases, $X(n_{i\alpha\sigma})$ tends to zero as $n^{1/3}_{i\alpha\sigma}(1-n_{i\alpha\sigma})^{1/3}$ for $n_{i\alpha\sigma}\to 0$ or 1, as corresponds to the conventional exchange energy in this limit $E^{X}_{i\alpha}\to -Kn^{4/3}_{i\alpha\sigma}$, in the three-dimensional case for $n_{i\alpha\sigma}\to 0$.

It is also worth commenting that for a crystal with infinite coordination corresponding to the DMF limit,[24] the exchange hole becomes localized in the nearest-neighbor sites, $X(n_{i\alpha\sigma})=1$. In general, when the lattice coordination is increased over a given coordination number we can expect $X(n_{i\alpha\sigma})$ to increase towards 1.

Summarizing this discussion, the exchange energy can be written in the following way:

$$E^X[\{n_{i\alpha\sigma}\}]=-\frac{1}{2}\sum_{i\alpha\sigma}X(n_{i\alpha\sigma})J_{i\alpha}^{\mathrm{NN}}n_{i\alpha\sigma}(1-n_{i\alpha\sigma}), \quad (16)$$

where for most practical cases, $X(n_{i\alpha\sigma})$ can be taken constant. Then, we can introduce the following exchange potential $V_{i\alpha\sigma}^X$:

$$V_{i\alpha\sigma}^X=\frac{\partial E^X[\{n_{i\alpha\sigma}\}]}{\partial n_{i\alpha\sigma}}=-X(n_{i\alpha\sigma})J_{i\alpha}^{\mathrm{NN}}\left(\frac{1}{2}-n_{i\alpha\sigma}\right). \quad (17)$$

One should keep in mind that for $n_{i\alpha\sigma}$ close to 0 or 1, $X(n_{i\alpha\sigma})$ cannot be assumed to be constant and Eq. (17) should be modified accordingly including the contribution of the derivative of $X(n_{i\alpha\sigma})$ with respect to $n_{i\alpha\sigma}$.

C. Correlation energy

In a first step, we discuss extra-atomic contributions to the correlation energy. These contributions arise due to the extra-atomic screening of the exchange interaction and the Coulomb-hole energy.[7,8] As discussed in Ref. 26, we can embody all these effects in a factor $\gamma(n_{i\alpha\sigma})$ such that the sum of the exchange and extra-atomic correlation energies $\tilde{E}^{\mathrm{XC}}$, is given by

$$\tilde{E}^{\mathrm{XC}}[\{n_{i\alpha\sigma}\}]=-\frac{1}{2}\sum_{i\alpha\sigma}\gamma(n_{i\alpha\sigma})X(n_{i\alpha\sigma})J_{i\alpha}^{\mathrm{NN}}n_{i\alpha\sigma}(1-n_{i\alpha\sigma}). \quad (18)$$

We have also found in Ref. 26 that for $0.15<n_{i\alpha\sigma}<0.85$, the product $\gamma(n_{i\alpha\sigma})X(n_{i\alpha\sigma})$ is very well approximated by 1. This suggests replacing $\gamma(n_{i\alpha\sigma})$ by a constant $\gamma_{i\alpha\sigma}$ defined by the condition $\gamma_{i\alpha\sigma}X(n_{i\alpha\sigma})=1$ for the occupancy range $0.15<n_{i\alpha\sigma}<0.85$ and write for the whole interval $0<n_{i\alpha\sigma}<1$

$$\tilde{E}^{\mathrm{XC}}[\{n_{i\alpha\sigma}\}]=-\frac{1}{2}\sum_{i\alpha\sigma}\gamma_{i\alpha\sigma}X(n_{i\alpha\sigma})J_{i\alpha}^{\mathrm{NN}}n_{i\alpha\sigma}(1-n_{i\alpha\sigma}). \quad (19)$$

This equation defines, in our formalism, the exchange and extra-atomic correlation energy. Notice that in the DMF approximation $X(n_{i\alpha\sigma})=1$ and also $\gamma_{i\alpha\sigma}=1$. Then, $\tilde{E}^{\mathrm{XC}}$ is well approximated in this limit by

$$\tilde{E}^{\mathrm{XC}}[\{n_{i\alpha\sigma}\}]=-\frac{1}{2}\sum_{i\alpha\sigma}J_{i\alpha}^{\mathrm{NN}}n_{i\alpha\sigma}(1-n_{i\alpha\sigma}); \quad (20)$$

this simply reflects that no extra-atomic correlation term contributes to the many-body energy in the DMF limit. This can be easily understood as the result of having, in the DMF approximation, all the exchange hole localized in the nearest-neighbor sites: extra-atomic screening can not reallocate this hole that has already approached the $i\alpha\sigma$ orbital to its nearest neighbor's distance. We should also comment that the many-body potential $\tilde{V}_{i\alpha,\sigma}^{\mathrm{XC}}$, associated with $\tilde{E}^{\mathrm{XC}}$ is given by

$$\tilde{V}_{i\alpha,\sigma}^{\mathrm{XC}}=\frac{\partial\tilde{E}^{\mathrm{XC}}[\{n_{i\alpha\sigma}\}]}{\partial n_{i\alpha\sigma}}=-\gamma_{i\alpha\sigma}X(n_{i\alpha\sigma})J_{i\alpha}^{\mathrm{NN}}\left(\frac{1}{2}-n_{i\alpha\sigma}\right), \quad (21)$$

where $X(n_{i\alpha\sigma})$ has been assumed to be practically constant.

Let us now consider the intra-atomic correlation energy. As discussed in Ref. 26, intra-atomic correlation effects appear when part of the total exchange-correlation hole $(1-n_{i\alpha\sigma})$ in Eq. (20), is transferred to the same atom i of the $i\alpha\sigma$ orbital. Assume that a fraction $f_{i\alpha\sigma}(1-n_{i\alpha\sigma})$ with $0<f_{i\alpha\sigma}<1$, is transferred to the atom i. Then, the intratomic correlation energy associated with the $i\alpha\sigma$ orbital should be given by

$$E_{I,i\alpha\sigma}^C=-\frac{f_{i\alpha\sigma}}{2}U_in_{i\alpha\sigma}(1-n_{i\alpha\sigma}). \quad (22)$$

At the same time, the extra-atomic exchange-correlation energy should be reduced by a factor $(1-f_{i\alpha\sigma})$, due to the smaller hole located outside the atom. Then, the total exchange-correlation energy should be given, in the DMF limit, by

$$E^{\mathrm{XC}}[\{n_{i\alpha\sigma}\}]=-\frac{1}{2}\sum_{i\alpha\sigma}(1-f_{i\alpha\sigma})J_{i\alpha}^{\mathrm{NN}}n_{i\alpha\sigma}(1-n_{i\alpha\sigma})-\frac{1}{2}\sum_{i\alpha\sigma}f_{i\alpha\sigma}U_in_{i\alpha\sigma}(1-n_{i\alpha\sigma}). \quad (23)$$

This equation shows that intra-atomic correlation effects can be added to the extra-atomic exchange-correlation energy by considering an effective interaction $(U_i-J_{i\alpha}^{\mathrm{NN}})$ inside the local site i. This result suggests introducing the following ''reduced'' Hubbard Hamiltonian:

$$\hat{H}^r=\sum_{i\alpha\sigma}[E_{i\alpha}^{\sigma}+\tilde{V}_{i\alpha,\sigma}^H+\tilde{V}_{i\alpha,\sigma}^{XC}]\hat{n}_{i\alpha,\sigma}+\sum_{i\alpha\neq j\beta,\sigma}t_{i\alpha,j\beta}\hat{c}_{i\alpha,\sigma}^{\dagger}\hat{c}_{j\beta,\sigma}+\frac{1}{2}\sum_{i,\alpha\sigma\neq\beta\sigma'}\tilde{U}_i\hat{n}_{i\alpha\sigma}\hat{n}_{i\beta\sigma'}, \quad (24)$$

already mentioned in the Introduction, where $\tilde{V}_{i\alpha,\sigma}^H=\Sigma_{\beta\sigma'\neq\alpha\sigma}J_i^{\mathrm{NN}}n_{i\beta\sigma'}+\Sigma_{j\neq i}{}^{\beta\sigma'}J_{i\alpha,j\beta}n_{j\beta,\sigma'}$; in Eq. (24) the exchange and extraatomic correlation effects are included in the local potential $\tilde{V}_{i\alpha,\sigma}^{\mathrm{XC}}$, while $\tilde{U}_i$ is the effective intra-atomic Coulomb interaction $(U_i-J_i^{\mathrm{NN}})$, assuming $J_{i\alpha}^{\mathrm{NN}}$ to be α independent. Notice that the total Hartree potential $V_{i\alpha,\sigma}^H$, associated with Eq. (8) is given by $\tilde{V}_{i\alpha,\sigma}^H+\Sigma_{\beta\sigma'\neq\alpha\sigma}\tilde{U}_in_{i\beta\sigma'}$ as it should be. For a Hubbard Hamiltonian such that $U_i=J_i^{\mathrm{NN}}$, Eq. (24) already represents the effective LD-Hamiltonian Eq. (6). Our first important result is to approximate Hamiltonian (1) by Eq. (24), where the LD potentials, $\tilde{V}_{i\alpha,\sigma}^H$ and $\tilde{V}_{i\alpha,\sigma}^{\mathrm{XC}}$, should be treated, regarding total energies, such as the many-body term $V_{i\alpha,\sigma}^{\mathrm{MB}}$ in Eq. (6).

In the following section we concentrate our analysis on discussing the many-body properties of the restricted Hub-

bard Hamiltonian given by Eq. (24). We shall present solutions to this Hamiltonian using a LD approximation and a many-body approach. In the LD approximation $\frac{1}{2}\Sigma_{i,\alpha\sigma\neq\beta\sigma'}\tilde{U}_i\hat{n}_{i\alpha\sigma}\hat{n}_{i\beta\sigma'}$ is replaced by a Hartree energy and a correlation energy $E^I[\{n_{i\alpha\sigma}\},\tilde{U}_i,t_{ij}]$, a function of the occupation numbers set $\{n_{i\alpha\sigma}\}$, and the parameters $\tilde{U}_i$ and t_{ij}. In the second approach, we introduce a *local* self-energy $\Sigma_{ii}(\omega)$ and calculate correlation energies and density of states using conventional Green's function methods. We should comment that in this last approach we neglect off-diagonal self-energies $\Sigma_{ij}(\omega)$, that one can expect to be small. This is exact in the DMF limit, with a lattice having infinite coordination number; in this case it has been shown[27] that $\Sigma_{ij}(\omega)\to 0$ and only diagonal self-energies contribute to the electronic properties of the system. One should keep in mind that this is a fundamental approximation in our approach and that, accordingly, for low-dimensional cases with low coordination our solution may fail (regarding this point, see the discussion in Sec. V). As our two methods, the LD and the self-energy approaches, are obviously linked through the correlation energy, we discuss both solutions together in the next section.

III. ANALYSIS OF THE RESTRICTED HUBBARD HAMILTONIAN

Our starting point in this section is the ''reduced'' Hubbard Hamiltonian

$$\hat{H}^r=\sum_{i\alpha\sigma}\tilde{E}^{\sigma}_{i\alpha}\hat{n}_{i\alpha\sigma}+\sum_{i\alpha\neq j\beta,\sigma}t_{i\alpha,j\beta}\hat{c}^{\dagger}_{i\alpha\sigma}\hat{c}_{j\beta\sigma}+\frac{1}{2}\sum_{i\alpha\sigma\neq\beta\sigma'}\tilde{U}_i\hat{n}_{i\alpha\sigma}\hat{n}_{i\beta\sigma'}, \tag{25}$$

where we define $\tilde{E}^{\sigma}_{i\alpha}=E^{\sigma}_{i\alpha}+\tilde{V}^{H}_{i\alpha\sigma}+\tilde{V}^{\mathrm{XC}}_{i\alpha\sigma}$ in Eq. (25). We look for a solution of Hamiltonian (25) by using Green-function techniques and introducing diagonal self-energies $\Sigma^{i\sigma}_{\alpha\alpha}(\omega)$. This implies neglecting off-diagonal contributions, as corresponds to the DMF approximation.

A. Self-energy approach

Our first goal is to find an appropriate self-energy $\Sigma^{\sigma}_{i\alpha\alpha}(\omega)$ for describing many-body effects within this model. This self-energy $\Sigma^{\sigma}_{i\alpha\alpha}$ allows us to calculate different densities of states $\rho^{\sigma}_{j\alpha,k\beta}$ defining the following Green function $G^{\sigma}_{j\alpha,k\beta}$:

$$G^{\sigma}_{j\alpha,k\beta}(\omega)=[\omega\boldsymbol{\delta}-\boldsymbol{H}^{\sigma}]^{-1}_{j\alpha,k\beta}, \tag{26}$$

here $\boldsymbol{\delta}$ is the identity matrix and

$$H^{\sigma}_{j\alpha,k\beta}=(\tilde{E}^{\sigma,H}_{j\alpha}+\Sigma^{\sigma}_{i\alpha\alpha})\,\delta_{\alpha\beta}\delta_{jk}+t^{\sigma}_{j\alpha,k\beta} \tag{27}$$

with $\tilde{E}^{\sigma,H}_{j\alpha}=\tilde{E}^{\sigma}_{j\alpha}+\tilde{U}_j\Sigma_{\beta\sigma'\neq\alpha\sigma}n_{j\beta\sigma'}$; then $\rho^{\sigma}_{j\alpha,k\beta}(\omega)$ is given by

$$\rho^{\sigma}_{j\alpha,k\beta}(\omega)=-\frac{1}{\pi}ImG^{\sigma}_{j\alpha,k\beta}(\omega). \tag{28}$$

Total energies and other quantities can be calculated using conventional Green-function methods. In particular, the total energy associated with Hamiltonian (25) is given by

$$E=-\frac{1}{2}\sum_{ij\alpha\beta\sigma}\mathrm{Im}\int_{-\infty}^{E_F}(\omega\delta_{i\alpha,j\beta}+\tilde{E}^{\sigma}_{j\alpha}\delta_{i\alpha,j\beta}+t^{\sigma}_{i\alpha,j\beta})\times G_{j\beta,i\alpha}(\omega)\frac{d\omega}{2\pi}. \tag{29}$$

The calculation of $\Sigma^{\sigma}_{i\alpha\alpha}(\omega)$ is based on an interpolative approach,[28–31] which follows the following.

(i) First, we look for $\Sigma^{\sigma}_{i\alpha\alpha}(\omega)$ in the limit $\tilde{U}_i\gg t$. This is the atomic limit that can be calculated exactly.

(ii) In a second step, we calculate the second-order self-energy $\Sigma^{\sigma(2)}_{i\alpha\alpha}(\omega)$ using as the expansion parameter $\tilde{U}_i/t$.

(iii) Third, we look for an interpolative self-energy that yields the correct limits for $\tilde{U}_i/t\gg 1$ (atomic) and $\tilde{U}_i/t\ll 1$ (second-order perturbative expansion).

(iv) The effective levels and correlation functions necessary for the determination of $\Sigma^{\sigma}_{i\alpha\alpha}(\omega)$ are calculated imposing self-consistency conditions.

1. Atomic limit

Let us first consider the atomic limit $\tilde{U}_i/t\gg 1$. For this case, it is sufficient to consider the atomic Hamiltonian

$$\hat{H}^{at}=\sum_{\alpha\sigma}\tilde{E}^{\sigma}_{i\alpha}\hat{n}_{i\alpha\sigma}+\frac{1}{2}\tilde{U}_i\sum_{\alpha\sigma\neq\beta\sigma'}\hat{n}_{i\alpha\sigma}\hat{n}_{i\beta\sigma'}. \tag{30}$$

In Appendix A, we show how to calculate the one-body Green's functions of this Hamiltonian, using the equation of motion technique. This procedure yields the following atomic result

$$G^{(at)\sigma}_{i\alpha\alpha}(\omega)=\frac{\left\langle\prod_{\beta\sigma'\neq\alpha\sigma}(1-\hat{n}_{i\beta\sigma'})\right\rangle}{\omega-\tilde{E}^{\sigma}_{i\alpha}+i0^{+}}+\sum_{\beta\sigma'\neq\alpha\sigma}\frac{\left\langle\hat{n}_{i\beta\sigma'}\prod_{(\gamma\sigma''\neq i\beta\sigma')\neq\alpha\sigma}(1-\hat{n}_{i\gamma\sigma''})\right\rangle}{\omega-\tilde{E}^{\sigma}_{i\alpha}-\tilde{U}_i+i0^{+}}+\cdots+\frac{\left\langle\prod_{\beta\sigma'\neq\alpha\sigma}\hat{n}_{i\beta\sigma'}\right\rangle}{\omega-\tilde{E}^{\sigma}_{i\alpha}-(2M-1)\tilde{U}_i+i0^{+}}, \tag{31}$$

where $2M$ is the degeneracy of the $i\alpha\sigma$ levels. In this expression all possible charge states of the atom give a contribution to $G^{(at)\sigma}_{i,\alpha\alpha}$. Its evaluation requires the knowledge of the many particle correlations $\langle\hat{n}_{i\alpha\sigma}\hat{n}_{i\beta\sigma'}\rangle$, $\langle\hat{n}_{i\alpha\sigma}\hat{n}_{i\beta\sigma'}\hat{n}_{i\gamma\sigma''}\rangle$, etc. However, for sufficiently large $\tilde{U}_i$, fluctuations in the atom charge with respect to the mean charge $\mathcal{N}_i$, by more than one electron become negligible, and $G^{(at)\sigma}_{i,\alpha\alpha}(\omega)$ is accurately given by the three poles expression

$$G_{i,\alpha\alpha}^{(at)\sigma}\approx\frac{A_{N_i-1}^{\alpha}}{\omega-\tilde{E}_{i\alpha}^{\sigma}-\tilde{U}_i(N_i-1)+i0^+}+\frac{A_{N_i}^{\alpha}}{\omega-\tilde{E}_{i\alpha}^{\sigma}-\tilde{U}_iN_i+i0^+}+\frac{A_{N_i+1}^{\alpha}}{\omega-\tilde{E}_{i\alpha}^{\sigma}-\tilde{U}_i(N_i+1)+i0^+},\tag{32}$$

where $N_i=\mathrm{Int}[\mathcal{N}_i]$ and $\mathcal{N}_i=\Sigma_{\alpha\sigma}n_{i\alpha\sigma}$. In order to obtain the exact first three moments of Eq. (32), the weight factors $A_{N_i-1}^{\sigma}$, $A_{N_i}^{\sigma}$, and $A_{N_i+1}^{\sigma}$, should satisfy the following sum rules (see Appendix B):

$$A_{N_i-1}^{\alpha}+A_{N_i}^{\alpha}+A_{N_i+1}^{\alpha}=1,\tag{33}$$

$$(N_i-1)A_{N_i-1}^{\alpha}+N_iA_{N_i}^{\alpha}+(N_i+1)A_{N_i+1}^{\alpha}=\sum_{\beta\sigma'\neq\alpha\sigma}\langle\hat{n}_{i\beta\sigma'}\rangle,\tag{34}$$

$$(N_i-1)^2A_{N_i-1}^{\alpha}+N_i^2A_{N_i}^{\alpha}+(N_i+1)^2A_{N_i+1}^{\alpha}=\sum_{\beta\sigma'\neq\alpha\sigma}\langle\hat{n}_{i\beta\sigma'}\rangle+\sum_{(\beta\sigma'\neq\gamma\sigma'')\neq\alpha\sigma}\langle\hat{n}_{i\beta\sigma'}\hat{n}_{i\gamma\sigma''}\rangle.\tag{35}$$

Notice that Eqs. (32)–(35) define $G_{i\alpha\alpha}^{(at)\sigma}$ as a function of the mean charges $\langle\hat{n}_{i\beta\sigma'}\rangle$ and the two-body correlation functions $\langle\hat{n}_{i\alpha\sigma}\hat{n}_{i\beta\sigma'}\rangle$. From $G_{i\alpha\alpha}^{(at)\sigma}$, one can define an atomic self-energy using the equation

$$\Sigma_{i\alpha\alpha}^{(at)\sigma}=\omega-\tilde{E}_{i\alpha}^{\sigma H}-[G^{(at)\sigma}]_{i\alpha\alpha}^{-1},\tag{36}$$

where $\tilde{E}_{i\alpha}^{\sigma H}$ is the Hartree level. Using Eqs. (32)–(36), it can be shown that $\Sigma_{i\alpha\alpha}^{(at)\sigma}$ can be written as the ratio of two polynomials in ω of the form

$$\Sigma_{i\alpha\alpha}^{(at)\sigma}=\frac{a_{i\alpha}^{\sigma}\tilde{U}_i^2(\omega-\tilde{E}_{i\alpha}^{\sigma})+b_{i\alpha}^{\sigma}\tilde{U}_i^3}{(\omega-\tilde{E}_{i\alpha}^{\sigma}+i0^+)^2+c_{i\alpha}^{\sigma}\tilde{U}_i(\omega-\tilde{E}_{i\alpha}^{\sigma}+i0^+)+d_{i\alpha}^{\sigma}\tilde{U}_i^2},\tag{37}$$

where

$$a_{i\alpha}^{\sigma}=(\mathcal{N}_i-n_{i\alpha\sigma})[1-(\mathcal{N}_i-n_{i\alpha\sigma})]+\sum_{(\beta\sigma'\neq\gamma\sigma'')\neq\alpha\sigma}\langle\hat{n}_{i\beta\sigma'}\hat{n}_{i\gamma\sigma''}\rangle,\tag{38}$$

$$c_{i\alpha}^{\sigma}=\mathcal{N}_i-n_{i\alpha\sigma}-3N_i,\tag{39}$$

$$d_{i\alpha}^{\sigma}=\sum_{(\beta\sigma'\neq\gamma\sigma'')\neq\alpha\sigma}\langle\hat{n}_{i\beta\sigma'}\hat{n}_{i\gamma\sigma''}\rangle+3N_i^3-1-(3N_i-1)(\mathcal{N}_i-n_{i\alpha\sigma}),\tag{40}$$

$$b_{i\alpha}^{\sigma}=N_i^2(1-N_i)-(\mathcal{N}_i-n_{i\alpha\sigma})d_{i\alpha}^{\sigma}.\tag{41}$$

2. Second order perturbation self-energy

In the second step mentioned above, we calculate the second-order self-energy $\Sigma_{i,\alpha\alpha}^{\sigma(2)}(\omega)$. Conventional perturbation theory yields

$$\Sigma_{i\alpha\alpha}^{\sigma(2)}=\tilde{U}_i^2\sum_{\beta\sigma'\neq\alpha\sigma}\int_{-\infty}^{\infty}d\epsilon_1d\epsilon_2d\epsilon_3\times\frac{\rho_{i\alpha\sigma}(\epsilon_1)\rho_{i\beta\sigma'}(\epsilon_2)\rho_{i\beta\sigma'}(\epsilon_3)}{\omega+\epsilon_2-\epsilon_1-\epsilon_3+i0^+}[f_1f_3(1-f_2)+(1-f_1)(1-f_3)f_2],\tag{42}$$

where $f_i=f(\epsilon_i)$ denotes the Fermi distribution function, and $\rho_{i\beta\sigma'}(\omega)$ are effective densities of states given by Eqs. (26)–(28), taking effective levels $E_{i\alpha}^{\sigma,\mathrm{eff}}$ instead of $E_{i\alpha}^{\sigma,H}+\Sigma_{i\alpha\alpha}^{\sigma}$. The effective levels $E_{i\alpha}^{\sigma,\mathrm{eff}}$ in the $i$site are introduced to fulfill charge consistency conditions in the $i\alpha\sigma$ levels as explained below, and are closely related to the LD solution introduced in Sec. II. Before going into these important points, let us discuss how to get an interpolative self-energy $\Sigma_{i\alpha\alpha}^{\sigma}(\omega)$ between the two limits ($\tilde{U}_i/t\to0$ and $\tilde{U}_i/t\to\infty$) just presented.

3. Interpolative self-energy

This can be achieved noticing that

$$\Sigma_{i\alpha\alpha}^{\sigma(2)}(\omega)\to\tilde{U}_i^2\frac{\sum_{\beta\sigma'\neq\alpha\sigma}n_{i\beta\sigma'}(1-n_{i\beta\sigma'})}{\omega-E_{i\alpha}^{\sigma,\mathrm{eff}}}\tag{43}$$

when $t/\omega\to0$. On the other hand, if we take formally the limit $\tilde{U}_i\to0$ in Eq. (37), we see that

$$\Sigma_{i\alpha\alpha}^{\sigma(at)}\to\frac{a_{i\alpha}^{\sigma}\tilde{U}_i^2}{(\omega-\tilde{E}_{i\alpha}^{\sigma}+i0^+)}.\tag{44}$$

In this small $\tilde{U}_i$ limit, we can assume that $\langle\hat{n}_{i\beta\sigma'}\hat{n}_{i\gamma\sigma''}\rangle\approx n_{i\beta\sigma'}n_{i\gamma\sigma''}$. Then, $a_{i\alpha}^{\sigma}$ goes to $\Sigma_{\beta\sigma'\neq\alpha\sigma}n_{i\beta\sigma'}(1-n_{i\beta\sigma'})$, and

$$\Sigma_{i\alpha\alpha}^{\sigma(at)}\to\frac{\tilde{U}_i^2\sum_{\beta\sigma'\neq\alpha\sigma}n_{i\beta\sigma'}(1-n_{i\beta\sigma'})}{(\omega-\tilde{E}_{i\alpha}^{\sigma}+i0^+)}.\tag{45}$$

Equations (43) and (45) suggest to define the following interpolative self-energy, replacing $(\omega-E_{i\alpha}^{\sigma,\mathrm{eff}})$ by $\tilde{U}_i^2\Sigma_{\beta\sigma'\neq\alpha\sigma}n_{i\beta\sigma'}(1-n_{i\beta\sigma'})/\Sigma_{i\alpha\alpha}^{\sigma(2)}(\omega)$:

$$\Sigma_{i\alpha\alpha}^{\sigma}=\left(\frac{\Sigma_{i\alpha\alpha}^{\sigma(2)}}{h_{i\alpha}^{\sigma}}\right)\frac{a_{i\alpha}^{\sigma}+(a_{i\alpha}^{\sigma}\Delta E_{i\alpha}^{\sigma}/\tilde{U}_i+b_{i\alpha}^{\sigma}/h_{i\alpha}^{\sigma})(\Sigma_{i\alpha\alpha}^{\sigma(2)}/\tilde{U}_i)}{1+(2\Delta E_{i\alpha}^{\sigma}/\tilde{U}_i+c_{i\alpha}^{\sigma})(\Sigma_{i\alpha\alpha}^{\sigma(2)}/h_{i\alpha}^{\sigma}\tilde{U}_i)+(c_{i\alpha}^{\sigma}\Delta E_{i\alpha}^{\sigma}/\tilde{U}_i+d_{i\alpha}^{\sigma})(\Sigma_{i\alpha\alpha}^{\sigma(2)}/h_{i\alpha}^{\sigma}\tilde{U}_i)^2},\tag{46}$$

where

$$h_{i\alpha}^{\sigma}=\sum_{\beta\sigma'\neq\alpha\sigma} n_{i\beta\sigma'}(1-n_{i\beta\sigma'}) \tag{47}$$

and

$$\Delta E_{i\alpha}^{\sigma}=E_{i\alpha}^{\sigma,\mathrm{eff}}-\tilde{E}_{i\alpha}^{\sigma}. \tag{48}$$

Notice that Eq. (46) yields (a) for $\tilde{U}_i\rightarrow 0$, $\Sigma_{i\alpha\alpha}^{\sigma}\rightarrow\Sigma_{i\alpha\alpha}^{\sigma(2)}$, because $\Delta E_{i\alpha}^{\sigma}$ and $\Sigma_{i\alpha\alpha}^{\sigma(2)}/\tilde{U}_i$ goes to zero as $\tilde{U}_i$ and $h_{i\alpha}^{\sigma}$ goes to $a_{i\alpha}^{\sigma}$. (b) On the other hand, for $\tilde{U}_i/t\rightarrow\infty$, $\Sigma_{i\alpha\alpha}^{\sigma(2)}$ can be replaced by $\tilde{U}_i^2 h_{i\alpha}^{\sigma}/(\omega-E_{i\alpha}^{\sigma,\mathrm{eff}})$ and $\Sigma_{i\alpha\alpha}^{\sigma}$ then goes to the atomic limit.

4. Self-consistency conditions

The final step in order to determine $\Sigma_{i\alpha\alpha}^{\sigma}(\omega)$ is to calculate $n_{i\beta\sigma}$, the correlation functions $\langle\hat{n}_{i\alpha\sigma}\hat{n}_{i\beta\sigma'}\rangle$ and the effective levels $E_{i\alpha}^{\sigma,\mathrm{eff}}$ self-consistently. The charges and the correlation functions are determined through the relations

$$n_{i\alpha\sigma}=-\frac{1}{\pi}\int_{-\infty}^{\infty} f(\omega)\,\mathrm{Im}\,G_{i\alpha\alpha}^{\sigma}(\omega)\,d\omega, \tag{49}$$

$$\sum_{\beta\sigma'\neq\alpha\sigma}\langle\hat{n}_{i\alpha\sigma}\hat{n}_{i\beta\sigma'}\rangle=\sum_{\beta\sigma'\neq\alpha\sigma} n_{i\alpha\sigma}n_{i\beta\sigma'}-\frac{1}{\pi\tilde{U}_i}\int_{-\infty}^{\infty} f(\omega)\,\mathrm{Im}[\Sigma_{i\alpha\alpha}^{\sigma}(\omega)\times G_{i\alpha\alpha}^{\sigma}(\omega)]\,d\omega \tag{50}$$

that follow from the general equations satisfied by $\Sigma_{i\alpha\alpha}^{\sigma}$ and $G_{i\alpha\alpha}^{\sigma}$. We should comment that $\Sigma_{(\beta\sigma'\neq\gamma\sigma')\neq\alpha\sigma}\langle\hat{n}_{i\beta\sigma'}\hat{n}_{i\gamma\sigma''}\rangle$ in Eqs. (38) and (40) can be obtained from Eq. (50) in the following way:

$$\sum_{(\beta\sigma'\neq\gamma\sigma'')\neq\alpha\sigma}\langle\hat{n}_{i\beta\sigma'}\hat{n}_{i\gamma\sigma''}\rangle=\sum_{\gamma\sigma''\neq\beta\sigma'}\langle\hat{n}_{i\beta\sigma'}\hat{n}_{i\gamma\sigma''}\rangle-2\sum_{\beta\sigma'\neq\alpha\sigma}\langle\hat{n}_{i\beta\sigma'}\hat{n}_{i\alpha\sigma}\rangle. \tag{51}$$

It is important to stress that the self-consistent determination of the two-body correlation functions $\langle\hat{n}_{i\beta\sigma'}\hat{n}_{i\gamma\sigma''}\rangle$, is an essential ingredient of our approach for calculating $\Sigma_{i\alpha\alpha}^{\sigma}$. In other words, the atomic self-energy given by Eq. (37) depends not only on the self-consistent charge $n_{i\alpha\sigma}$ but on the self-consistent correlation functions $\Sigma_{\gamma\sigma''\neq\beta\sigma'}\langle\hat{n}_{i\beta\sigma'}\hat{n}_{i\gamma\sigma''}\rangle$. These self-consistent parameters introduce in the interpolative self-energy $\Sigma_{i\alpha\alpha}^{\sigma}(\omega)$, enough flexibility to yield an appropriate interpolation between the atomic and second order perturbation self-energies.

Finally, the effective levels $E_{i\alpha}^{\sigma,\mathrm{eff}}$ are chosen to fulfill the charge consistency between the value given by Eq. (49) and the ones defined by the effective one-electron Hamiltonian:

$$H_{j\alpha,k\beta}^{\mathrm{eff}}=E_{j\alpha}^{\sigma,\mathrm{eff}}\delta_{j\alpha,k\beta}+t_{j\alpha,k\beta}. \tag{52}$$

This condition guarantees that $\Sigma_{i\alpha\alpha}^{\sigma(2)}$ tends to the right limit when $\omega\rightarrow\infty$:

$$\Sigma_{i\alpha\alpha}^{\sigma(2)}\rightarrow\tilde{U}_i^2\frac{\sum_{\beta\sigma'\neq\alpha\sigma} n_{i\beta\sigma'}(1-n_{i\beta\sigma'})}{\omega-E_{i\alpha}^{\sigma,\mathrm{eff}}}. \tag{53}$$

In this one-electron Hamiltonian, $E_{j\alpha}^{\sigma,\mathrm{eff}}$ plays the role of an effective level that substitutes for $[\tilde{E}_{i\alpha}^{\sigma,H}+\Sigma_{i\alpha\alpha}^{\sigma}(\omega)]$ in Hamiltonian (27). When we compare Hamiltonian (52) with Hamiltonian (25), we realize that $E_{i\alpha}^{\sigma,\mathrm{eff}}$ plays the role of the following local-density level:

$$\tilde{E}_{i\alpha}^{\sigma,H}+\frac{\partial E^I[\{n_{i\alpha\sigma}\}]}{\partial n_{i\alpha\sigma}}, \tag{54}$$

where E^I is the correlation energy associated with the many-body term $1/2\Sigma_{i\beta\sigma'\neq\alpha\sigma}\tilde{U}_i\hat{n}_{i\alpha\sigma}\hat{n}_{i\beta\sigma'}$.

Notice that $E_{i\alpha}^{\sigma,\mathrm{eff}}$ should be determined to give the same local charge $n_{i\alpha\sigma}$ as the exact problem and this shows that

$$E_{i\alpha}^{\sigma,\mathrm{eff}}=\tilde{E}_{i\alpha}^{\sigma,H}+\frac{\partial E^I[\{n_{i\alpha\sigma}\}]}{\partial n_{i\alpha\sigma}}. \tag{55}$$

In other words, the effective Hamiltonian (52) we have to use to calculate the effective density of states $\rho_{i\alpha\sigma}(\omega)$ is nothing else that the LD approximation associated with the Hubbard Hamiltonian (25). It should be noted that, in order to calculate $E_{i\alpha}^{\sigma,\mathrm{eff}}$ using Eq. (55), one needs $E^I[\{n_{i\alpha\sigma}\}]$, a task that we address in the next section.

An alternative approach is to calculate $E_{i\alpha}^{\sigma,\mathrm{eff}}$ directly imposing charge consistent conditions as mentioned above. This consistency can also be written using Friedel-sum rules and Ward identities.[32] In particular, as shown in Ref. 30, one can replace charge consistent conditions by the following equation:

$$\int_{-\infty}^{\infty} f(\omega)\,\mathrm{Im}\left[G_{i\alpha\alpha}^{\sigma}(\omega)\frac{\partial\Sigma_{i\alpha\alpha}^{\sigma}}{\partial\omega}\right]d\omega=0 \tag{56}$$

which at zero temperature reduces to the Luttinger theorem,[33] ensuring fulfillment of the Friedel sum rule.

Summarizing this discussion: the effective level $E_{i\alpha}^{\sigma,\mathrm{eff}}$ is introduced to calculate the effective density of states $\rho_{i\alpha\sigma}(\omega)$, the quantity defining $\Sigma_{i\alpha\sigma}^{\sigma(2)}$; that level can be determined using two complementary approaches: (i) in the first one, $E_{i\alpha}^{\sigma,\mathrm{eff}}$ is given by the LD level of Eq. (55). In this approach we need to know the functional $E^I[\{n_{i\alpha\sigma}\}]$. (ii) In the second approach, $E_{i\alpha}^{\sigma,\mathrm{eff}}$ is calculated using Eq. (56). This second solution can always be applied to any general case and does not depend on the previous knowledge of the correlation energy associated with the local Hubbard term $1/2\tilde{U}_i\Sigma_{i,\alpha\sigma\neq\beta\sigma'}n_{i\alpha\sigma}n_{i\beta\sigma'}$.

We should comment that, were $E^I[\{n_{i\alpha\sigma}\}]$ known, one could obtain $E_{i\alpha}^{\sigma,\mathrm{eff}}$ more efficiently without having to use a self-consistent loop in the calculation. This justifies our interest in obtaining $E^I[\{n_{i\alpha\sigma}\}]$, as done in the next section.

It is interesting to mention that, as shown by Georges *et al.* (see Ref. 24), one can obtain a better description of the density of states of our system by changing slightly the pre-

scription to calculate $\rho_{i\alpha\beta}(\omega)$ in $\Sigma^{\sigma(2)}_{i\alpha\alpha}$. This approach offers a very convenient way of calculating Mott transitions in Hubbard Hamiltonians. The idea is to define a new density of states $\tilde{\rho}_{i\alpha\beta}(\omega)$ that incorporates in a more appropriate way the effect of the environment. This is achieved by introducing in the effective Hamiltonian defining the local density of states $\tilde{\rho}_{i\alpha\beta}(\omega)$ the local self-energy $\Sigma^{\sigma}_{j\beta\beta}$ in all the j sites, *save the same site i* where we are calculating $\tilde{\rho}_{i\alpha\beta}(\omega)$. We should mention that this procedure introduces a new self-consistent loop in the calculation, since $\tilde{\rho}_{i\alpha\beta}$ depends on $\Sigma^{\sigma}_{j\beta\beta}$, a quantity that depends on $\Sigma^{(2)\sigma}_{j\beta\beta}$, itself a function of $\tilde{\rho}_{i\alpha\beta}$.

B. Correlation energy: $E^I[n_{i\alpha\sigma}]$

$E^I[\{n_{i\alpha\sigma}\}]$ has been calculated by analyzing Hamiltonian (25) in two limits: (i) first, we consider the case $\tilde{U}_i/t\to\infty$, the atomic limit, with the i site practically decoupled from the crystal; (ii) in a second step we analyze the case $\tilde{U}_i/t \to 0$. In this limit, we calculate $E^I[\{n_{i\alpha\sigma}\}]$, using second order perturbation theory.

Having studied these two cases, $\tilde{U}_i/t\to 0$ and ∞, we introduce an ansatz for $E^I[\{n_{i\alpha\sigma}\}]$ that interpolates between those two limits. This procedure follows the same strategy we have used to calculate $\Sigma^{\sigma}_{i\alpha\alpha}(\omega)$ and we can expect it to yield also a reasonable approximation for $E^I[\{n_{i\alpha\sigma}\}]$. We have checked that this is the case by analyzing simple clusters, where we can calculate $E^I[\{n_{i\alpha\sigma}\}]$ exactly.

1. $\tilde{U}_i/t\to\infty$: Atomic limit

We analyze this limit using the atomic Green function [Eq. (32)] and the following equation:

$$E^{e-e} = -\sum_{\alpha\sigma} \lim \int_{-\infty}^{E_F} (\omega - E^{\sigma}_{i\alpha}) G^{\sigma}_{i,\alpha\alpha}(\omega) \frac{d\omega}{2\pi} \qquad (57)$$

that yields the electron-electron Coulomb energy for an interacting electron gas. In the $\tilde{U}_i/t\to\infty$ limit, this energy coincides with the correlation energy we are interested in.

In Eq. (32), we calculate $A^{\alpha}_{N_i-1}$, $A^{\alpha}_{N_i}$, and $A^{\alpha}_{N_i+1}$ using Eqs. (33)–(35), (49), and (50); in Eq. (50) we can now use for $\Sigma^{\sigma}_{i,\alpha\alpha}(\omega)$ the atomic limit given by Eq. (37). This procedure yields the following results:

$$A^{\alpha}_{N_i-1} = \frac{N_i}{\mathcal{N}_i} n_{i\alpha\sigma}[1-(\mathcal{N}_i - N_i)], \qquad (58)$$

$$A^{\alpha}_{N_i} = (1-n_{i\alpha\sigma}) + (N_i - \mathcal{N}_i)\left[1 - \frac{2n_{i\alpha\sigma}}{\mathcal{N}_i}(1+N_i)\right], \qquad (59)$$

$$A^{\alpha}_{N_i+1} = (\mathcal{N}_i - N_i) - n_{i\alpha\sigma}(\mathcal{N}_i - N_i)\frac{1+N_i}{\mathcal{N}_i} \qquad (60)$$

valid only for $\tilde{U}_i/t\to\infty$. Then, we introduce these quantities in the atomic Green function and obtain the following correlation energy from Eq. (57):

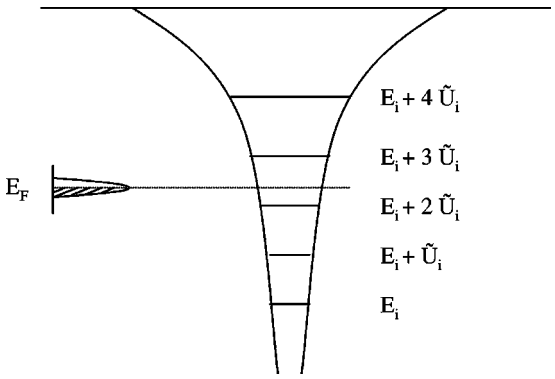

FIG. 1. Shows the atomic levels $E_i + \tilde{U}_i N_i$, associated with the atomic Hamiltonian (31). A continuum density of states is assumed to be much narrower than $\tilde{U}_i$.

$$E^I_{\text{atomic}}[\{n_{i\alpha\sigma}\}] = -\frac{1}{2}\tilde{U}_i \sum_{\alpha\sigma} n_{i\alpha\sigma}(1-n_{i\alpha\sigma}) + \frac{1}{2}\tilde{U}_i(\mathcal{N}_i - N_i)(1+N_i-\mathcal{N}_i). \qquad (61)$$

It is interesting to realize that the potential $V^I_{i\alpha\sigma}$ associated with this correlation energy is the following (remember that $\mathcal{N}_i = \Sigma_{\alpha\sigma} n_{i\alpha\sigma}$):

$$V^I_{i\alpha\sigma,\text{atomic}} = \frac{\partial E^I}{\partial n_{i\alpha\sigma}} = \tilde{U}_i(n_{i\alpha\sigma} - \mathcal{N}_i) + \tilde{U}_i N_i. \qquad (62)$$

This equation shows that the sum of the Hartree $\Sigma_{\beta\sigma'\neq\alpha\sigma}\tilde{U}_i n_{i\beta\sigma'}$ and the correlation potentials yields:

$$V^{\text{MB}}_{i\alpha\sigma,\text{atomic}} = \tilde{U}_i N_i, \qquad (63)$$

a not unexpected result, as this many-body level, $\tilde{U}_i N_i$, depends only on the integer number N_i. In other words, in the atomic limit electrons are transferred to the atom one by one: each time one electron enters the atom, the new many-body level controlling how another electron can be transferred to the atom jumps by $\tilde{U}_i$ due to the Coulomb repulsion the new electron has with any other atomic electron.

For the particular case that the atomic level $E_i + \tilde{U}_i N_i$, is resonating with a continuum density of states, electronic charge can be transferred to the atom: however, this mean charge transfer (less than one electron) cannot modify the atomic level as the electron jumping to the atom does not see itself. Figure 1 shows the different atomic levels of our model Hamiltonian and their possible distribution with respect to a continuum density of states, that is assumed to be much narrower that $\tilde{U}_i$.

Figure 2(a) shows E^I as a function of n_i for the degenerate case $n_i = n_{i\uparrow} = n_{i\downarrow} = \cdots n_{i\alpha\sigma}$ and four different levels; notice the discontinuity appearing in the derivative of $E^I[n_{i\alpha\sigma}]$ for $n_i = 1/4$, 2/4, 3/4, and 1 or, equivalently, for $N_i = 1$, 2, 3, and 4. Figure 2(b) shows $V^{\text{MB}}_{i\alpha\sigma}$ as a function of N_i for the same case; notice that this potential presents discontinuities of value $\tilde{U}_i$ for $N_i = 1,2,3$: this is in agreement with the general result of Perdew *et al.*[34] for an atom. Cases for atoms having more than four levels are similar to the ones shown in Fig. 2.

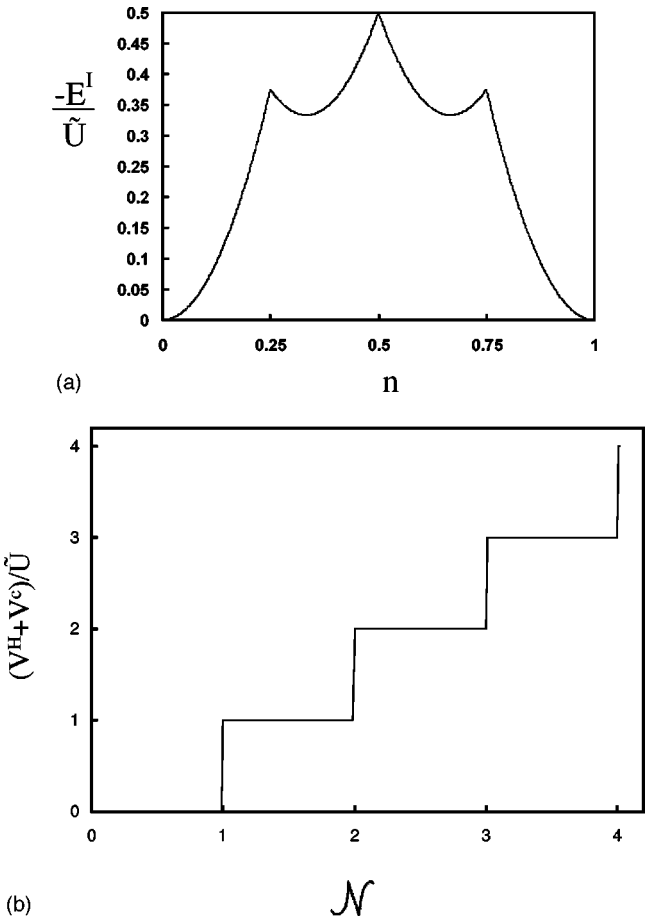

FIG. 2. (a) Correlation energy $(-E^I)$ as a function of n_i, in the atomic limit for $2M=4$. (b) The sum of the Hartree and the correlation energy is shown for the same case as a function of $\mathcal{N}$.

2. $\tilde{U}_i/t \to 0$. Perturbative calculation of $E^I[\{n_{i\alpha\sigma}\}]$

This limit can be analyzed using conventional perturbation theory. Figure 3 shows the different second order diagrams contributing, in the lowest order, to the correlation energy (first order diagrams contribute only to the Hartree energy). In the diagrams, electrons in the $i\alpha\sigma$ and $i\beta\sigma'$ states interact with each other creating virtual excitations that contribute to the correlation energy as follows:[35]

$$E^{I(2)}[\{n_{i\alpha\sigma}\}] = -\sum_i \left\{ \frac{\tilde{U}_i^2}{2} \sum_{\beta\sigma' \neq \alpha\sigma} \int_{-\infty}^{E_F} d\omega d\omega' \int_{E_F}^{\infty} d\omega'' d\omega''' \times \frac{\tilde{\rho}_{i\alpha\sigma}(\omega)\tilde{\rho}_{i\beta\sigma'}(\omega')\tilde{\rho}_{i\alpha\sigma}(\omega'')\tilde{\rho}_{i\beta\sigma'}(\omega''')}{\omega''+\omega'''-(\omega+\omega')} \right\}. \tag{64}$$

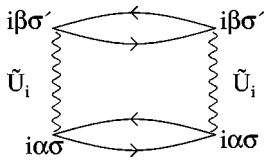

FIG. 3. Second order perturbative diagram contributing to E^I.

In Eq. (64), the sum extends upon all the possible values of $\alpha\sigma$ and $\beta\sigma'$, and the factor 1/2 is included to avoid double counting. Notice that $[(\omega''+\omega''')-(\omega+\omega')]$ represents the energy of the virtual excitation associated with two electrons occupying the $\alpha\sigma$ and $\beta\sigma'$ states, and having initial energies ω and ω' and final levels ω'' and ω''', respectively. This suggests to introduce the mean excitation energy $W_{\alpha\beta}$ associated with these virtual excitations and write for the second-order perturbation energy

$$E^{I(2)}[\{n_{i\alpha\sigma}\}] = -\sum_i \left\{ \frac{\tilde{U}_i^2}{2} \sum_{\beta\sigma' \neq \alpha\sigma} \frac{n_{i\alpha\sigma}(1-n_{i\alpha\sigma})n_{i\beta\sigma'}(1-n_{i\beta\sigma'})}{W_{\alpha\beta}} \right\}, \tag{65}$$

where we already find the functional dependence of $E^{I(2)}$ on $n_{i\alpha\sigma}$. We should comment, however, that $W_{\alpha\beta}$ itself also depends on $n_{i\alpha\sigma}$, introducing a complication in our discussion that we analyze below. For the time being, we shall assume $W_{\alpha\beta}$ to be known and discuss the interpolative expression we propose for calculating the correlation energy E^I for any value of $\tilde{U}/t$.

3. Interpolative correlation energy

The correlation energy we are interested in, E^I, has to yield Eq. (61) for $\tilde{U}/t \to \infty$ and Eq. (65) for $\tilde{U}/t \to 0$. This suggests, if $\mathcal{N}_i = N_i$ and hence the second term of Eq. (61) is zero, to use the following correlation energy:

$$E^I[\{n_{i\alpha\sigma}\}] = -\sum_i \left\{ \frac{1}{2}\tilde{U}_i \sum_{\alpha\sigma} n_{i\alpha\sigma}(1-n_{i\alpha\sigma})F(x) \right\}, \tag{66}$$

where $x = \Sigma_{\beta\sigma' \neq \alpha\sigma}(\tilde{U}_i/W_{\alpha\beta})n_{i\beta\sigma'}(1-n_{i\beta\sigma'})$, and $F(x)$ behaves in the following way:

$$F(x) = \begin{cases} x, & x \to 0, \\ 1, & x \to \infty. \end{cases} \tag{67}$$

These two limits yield the appropriate values of E^I for $\tilde{U}/t \to \infty$ and $\tilde{U}/t \to 0$.

We have found that a good approximation to $F(x)$ is

$$F(x) = a\frac{x}{1+x} + (1-a)(1-e^{-x}), \tag{68}$$

where a is a parameter fitted to the results discussed below for a cluster. The general correlation energy, for $\mathcal{N}_i \neq N_i$, is written as a generalization of Eq. (66) in the following way:

$$E^I[\{n_{i\alpha\sigma}\}] = -\sum_i \left\{ \frac{1}{2}\tilde{U}_i \sum_{\alpha\sigma} n_{i\alpha\sigma}(1-n_{i\alpha\sigma})F(x) + \frac{1}{2}\tilde{U}_i \times (\mathcal{N}_i - N_i)(1+N_i-\mathcal{N}_i)g\left(\frac{\tilde{U}_i}{W}, n_{i\alpha\sigma}; \mathcal{N}_i\right) \right\}, \tag{69}$$

where g should fulfill conditions

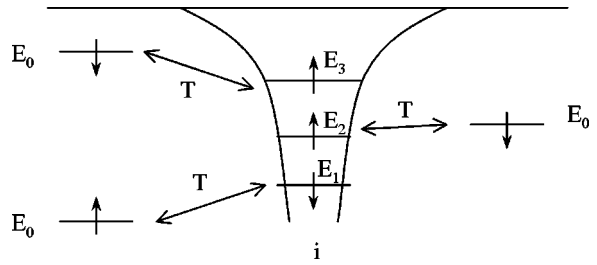

FIG. 4. Atomic model of $2\times(3)$ levels (including spin) interacting with three ''reservoirs'' simulated by three sharp levels.

$$g\rightarrow\begin{cases}0 & \text{faster than } \dfrac{\tilde{U}_i}{W} \text{ for } \tilde{U}_i\rightarrow 0,\\ 1 & \text{for } \tilde{U}_i\rightarrow\infty\end{cases} \tag{70}$$

in order to get the appropriate limits for E^I.

4. Simple models: Characterization of the parameters defining $E^I[\{n_{i\alpha\sigma}\}]$

We have determined a in Eq. (68) and the function g in Eq. (69), by analyzing the case shown in Fig. 4. Here, a single atom i with M levels α ($2M$ including spin) interacts with M independent levels m ($2M$ including spin). Each pair of levels can accommodate two electrons, with spins up and down, and all the electrons inside the atom interact with a Coulomb interaction $\tilde{U}_i$. The Hamiltonian describing this system is the following:

$$\hat{H}=\sum_{\alpha\sigma} E^{\sigma}_{i\alpha}\hat{n}_{i\alpha\sigma}+T\sum_{\alpha m\sigma}(\hat{c}^{\dagger}_{i\alpha\sigma}\hat{c}_{m\sigma}+\hat{c}^{\dagger}_{m\sigma}\hat{c}_{i\alpha\sigma})+\sum_{m\sigma} E_m\hat{n}_{m\sigma}+\frac{1}{2}\sum_{\alpha\sigma\neq\beta\sigma'}\tilde{U}_i\hat{n}_{i\alpha\sigma}\hat{n}_{i\beta\sigma'}. \tag{71}$$

The correlation energy $E^I[\{n_{i\alpha\sigma}\}]$, of this Hamiltonian can be obtained by solving, first Hamiltonian (71) exactly and, then, following the prescription given in Ref. 26, calculating the Hartree and the kinetic energy. Our results for $E^I[\{n_{i\alpha\sigma}\}]$ are presented in Fig. 5, taking : $n_i=n_{i\uparrow}=n_{i\downarrow}=\cdots n_{i\alpha\sigma}$ (all the occupancies of the different levels are equal), for different values of M ($M=1,2,3$ and 4), and $\tilde{U}_i/T$. For this particular case we have found that $E^I[\{n_{i\alpha\sigma}\}]$ can be well approximated by the following equation

$$E^I[\{n_{i\alpha\sigma}\}]=-\frac{b}{2}\tilde{U}_i\sum_{\alpha\sigma} n_{i\alpha\sigma}(1-n_{i\alpha\sigma})F(x)+\frac{1}{2}\tilde{U}_i(\mathcal{N}_i-N_i)(1+N_i-\mathcal{N}_i)F(y), \tag{72}$$

where

$$y=c\left(\frac{\tilde{U}_i}{T}\right)^2 n_{i\alpha\sigma}(1-n_{i\alpha\sigma})(\mathcal{N}_i-N_i)^{1/2}(1+N_i-\mathcal{N}_i)^{1/2},$$

$$x=\frac{\tilde{U}_i}{T}\sum_{\beta\sigma'\neq\alpha\sigma}\frac{n_{i\beta\sigma'}(1-n_{i\beta\sigma'})}{1/n^{1/2}_{i\alpha\sigma}(1-n_{i\alpha\sigma})^{1/2}+1/n^{1/2}_{i\beta\sigma'}(1-n_{i\beta\sigma'})^{1/2}},$$

and a, b, and c are parameters that have been fitted to the cluster solution. Table I gives the parameters used for the fit shown in Fig. 5.

In Eq. (72) we have used for x a dependence on $n_{i\beta\sigma'}(1-n_{i\beta\sigma'})$, apparently different from the one given above, after Eq. (66). One should realize, however, that in the atomic model we are considering (see Fig. 4), $W_{\alpha\beta}$ and T are related by the simple equation

$$W_{\alpha\beta}=\frac{T}{n^{1/2}_{i\alpha\sigma}(1-n_{i\alpha\sigma})^{1/2}}+\frac{T}{n^{1/2}_{i\beta\sigma'}(1-n_{i\beta\sigma'})^{1/2}}. \tag{73}$$

Replacing Eq. (73) into Eq. (66) yields the dependence of x we have introduced in Eq. (72).

In Eq. (72) we have also introduced the factor b to improve the fit to the results of the cluster model. On the other hand, the second term of the right hand side of Eq. (72) shows the appropriate limits for $\tilde{U}/T\rightarrow\infty$ and $\tilde{U}/T\rightarrow 0$. For $\tilde{U}/T\rightarrow\infty$, we recover the atomic limit, Eq. (61), while for $\tilde{U}/T\rightarrow 0$, this term contributes such as $\tilde{U}^2/T^3$, going to zero more rapidly than $\tilde{U}^2/T$ (the order of magnitude of the second order perturbation contribution).

Equation (72) and the parameters given in Table I define the correlation energy $E^I[\{n_{i\alpha\sigma}\}]$, for the particular case in which all the $2M$ levels have the same occupancy. In Fig. 5, we compare the exact values of E^I with our approximation, showing the quality of our fit. A more general correlation energy is needed, however, for cases in which the occupation numbers are different, as obtained by changing the relative energy of the atomic levels and their hoppings $T_{i\alpha}$.

This case can be obtained by generalizing the coefficients a and b, as well as the term $c[n_{i\alpha\sigma}(1-n_{i\alpha\sigma})/T^2]$, for values of $n_{i\alpha\sigma}\neq n_{i\beta\sigma}$ and $T_{i\alpha}\neq T_{i\beta}$. In Appendix C we discuss the details of our interpolative procedure; regarding our present purposes, let us only mention that, in this generalization, we replace the previous parameters by values $\langle a\rangle$, $\langle b\rangle$, and $\langle c[n_{i\alpha\sigma}(1-n_{i\alpha\sigma})/T^2_{i\alpha}]\rangle$, that interpolates between the cases presented in Fig. 5, with the new parameters written as a function of $n_{i\alpha\sigma}$ and $T_{i\alpha}$. Thus we find

$$E^I[\{n_{i\alpha\sigma}\}]=-\frac{\langle b\rangle}{2}\tilde{U}_i\sum_{\alpha\sigma} n_{i\alpha\sigma}(1-n_{i\alpha\sigma})F(\langle x_{i\alpha\sigma}\rangle)+\frac{1}{2}\tilde{U}_i(\mathcal{N}_i-N_i)(1+N_i-\mathcal{N}_i)F(\langle y\rangle). \tag{74}$$

$F(x)$ being given by $\{\langle a\rangle x/(1+x)+(1-\langle a\rangle)(1-\exp[-x])\}$, and

$$\langle y\rangle=\tilde{U}_i^2\left\langle c\frac{n_{i\alpha\sigma}(1-n_{i\alpha\sigma})}{T^2_{i\alpha}}\right\rangle(\mathcal{N}_i-N_i)^{1/2}(1+N_i-\mathcal{N}_i)^{1/2},$$

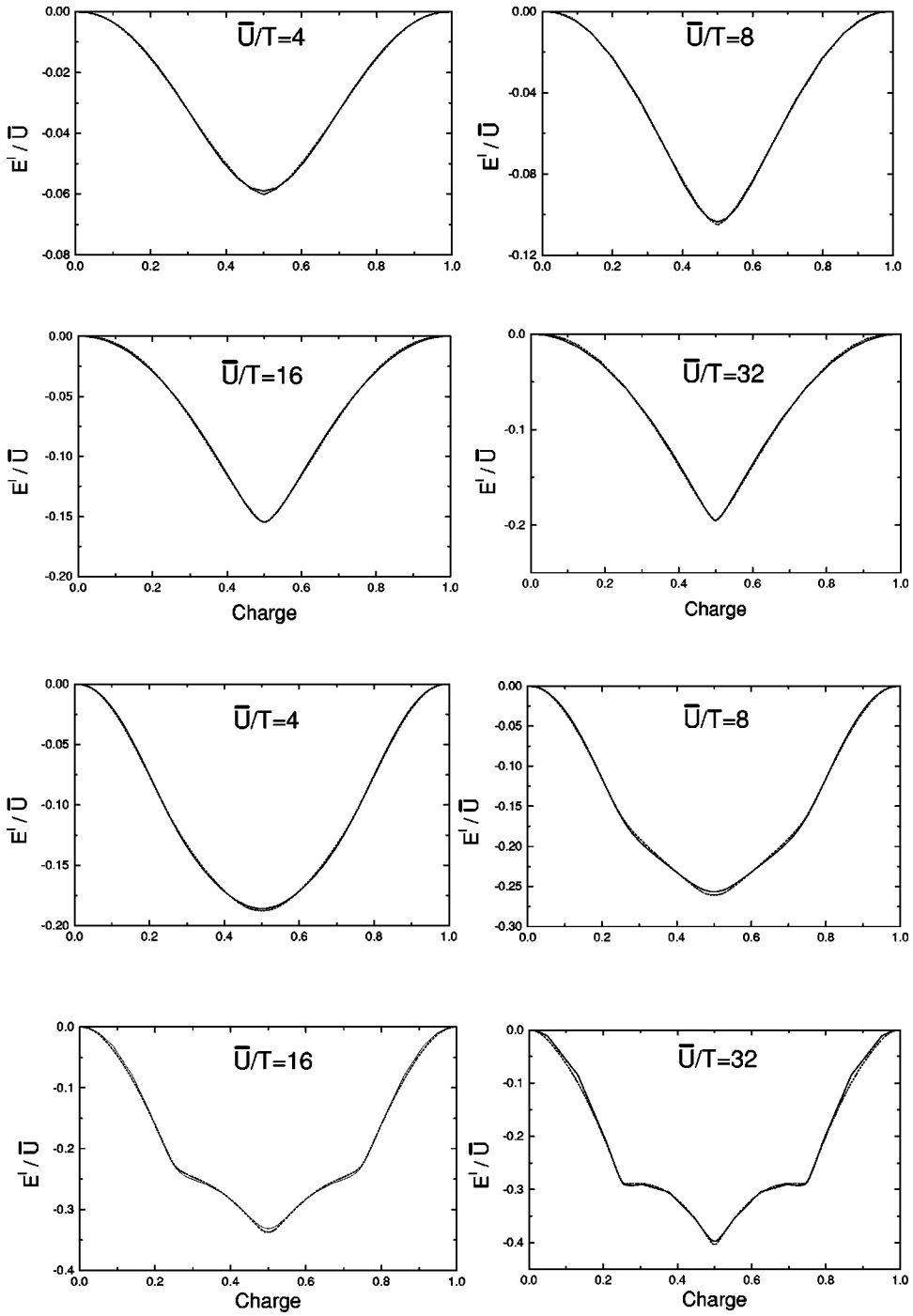

FIG. 5. $E^I/\tilde{U}$ as a function of n_i, for different $\tilde{U}/T$ values, as calculated exactly (full line) and using Eq. (72) (dashed line). (a) The first set of four figures correspond to the case $2M=2$; (b) the next four figures correspond to $2M=4$; (c) $2M=6$; (d) $2M=8$.

$$\langle x_{i\alpha\sigma}\rangle = \tilde{U}_i \sum_{\beta\sigma'(\neq\alpha\sigma)} \frac{n_{i\beta\sigma'}(1-n_{i\beta\sigma'})}{T_{i\alpha}/n_{i\alpha\sigma}^{1/2}(1-n_{i\alpha\sigma})^{1/2}+T_{i\beta}/n_{i\beta\sigma'}^{1/2}(1-n_{i\beta\sigma'})^{1/2}}.$$

We should stress that this equation applies to the simple model of Fig. 4. We can write Eq. (74) in a more convenient way by replacing $T_{i\alpha}$ by $W_{i\alpha}$, using Eq. (73), which is still true in the case $T_{i\alpha}\neq T_{i\beta}$. This yields the following correlation energy:

$$E^I[\{n_{i\alpha\sigma}\}] = -\frac{\langle b\rangle}{2}\tilde{U}_i \sum_{\alpha\sigma} n_{i\alpha\sigma}(1-n_{i\alpha\sigma})F(\widetilde{\langle x_{i\alpha\sigma}\rangle}) + \frac{1}{2}\tilde{U}_i(\mathcal{N}_i-N_i)(1+N_i-\mathcal{N}_i)F(\langle\tilde{y}\rangle), \tag{75}$$

where

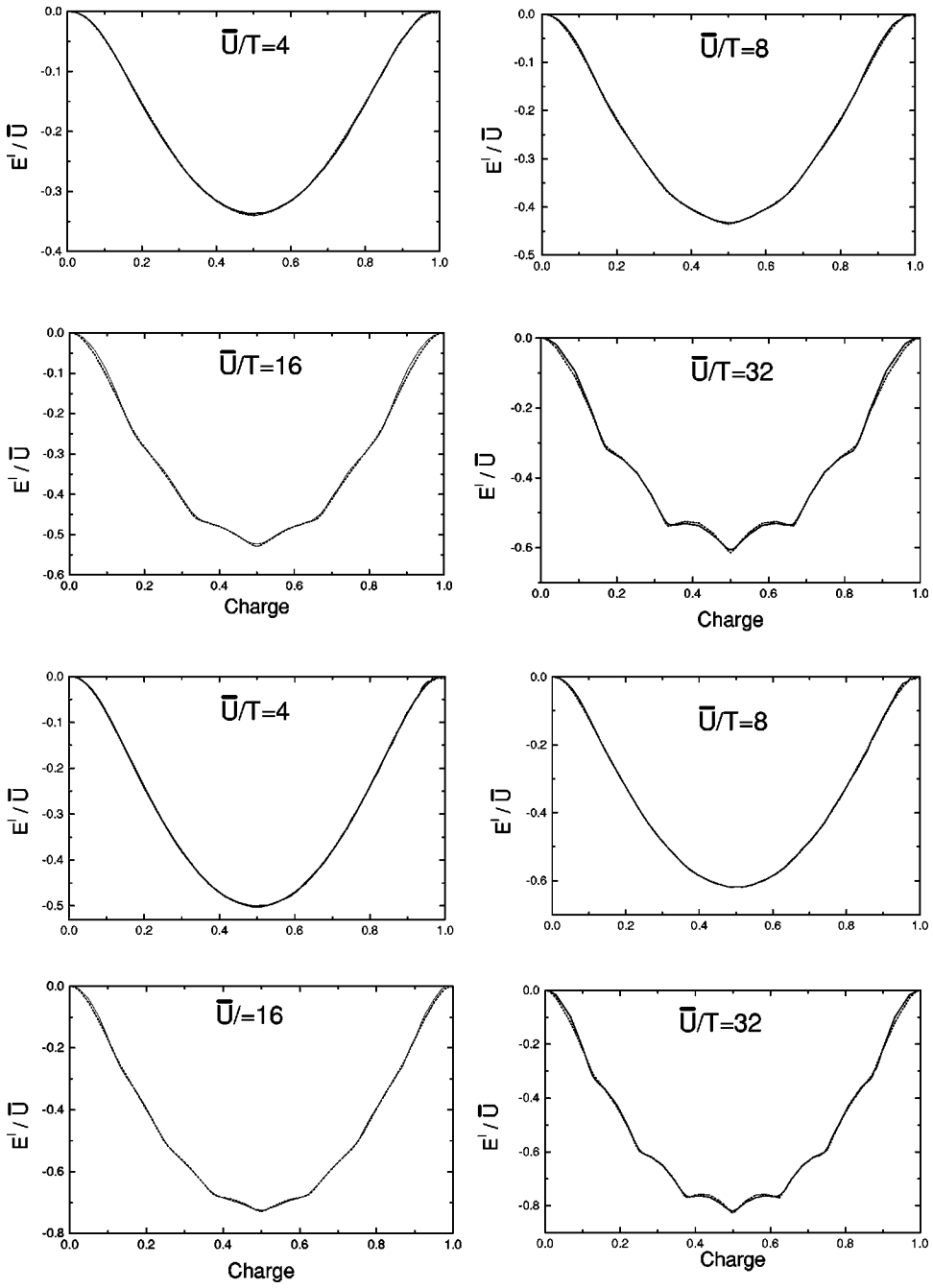

FIG. 5. (*Continued*).

$$\widetilde{\langle x_{i\alpha\sigma}\rangle} = \sum_{\beta\sigma'(\neq\alpha\sigma)} \frac{\tilde{U}_i}{W_{\alpha\beta}} n_{i\beta\sigma'}(1-n_{i\beta\sigma'}),$$

$$\langle \tilde{y} \rangle = \tilde{U}_i^2 \left\langle \frac{4c}{W_\alpha^2} \right\rangle (\mathcal{N}_i - N_i)^{1/2}(1+N_i-\mathcal{N}_i)^{1/2}.$$

In these equations $W_{\alpha\beta}=W_\alpha+W_\beta$, W_α representing the mean excitation energy between the empty and the occupied DOS associated with the orbital α.

IV. RESULTS FOR THE MULTILEVEL ANDERSON IMPURITY AND THE MULTIBAND HUBBARD LATTICE

In this section we analyze the properties of the multilevel Anderson model using the formalism discussed above. This model has been extensively used to represent a magnetic impurity in a metallic host[32] and more recently to simulate artificial atoms or quantum dots.[30,33,36–39]

As a first case we reconsider the model of Fig. 4, where an atom or quantum dot having a degeneracy $2M$, is connected to a reservoir. This model, with the reservoir simulated by sharp levels, can give us a rough idea of how the charge transfer between the quantum dot and the reservoir

TABLE I. Parameters a, b, and c in Eq. (72) used to fit E^I for $2M=2$, 4, 6, and 8.

U/T	a	b	c
		$2M=2$	
2	0.5	1.09	0.047
4	0.5	1.14	0.041
8	0.5	1.16	0.032
16	0.5	1.10	0.019
32	0.5	1.02	0.010
		$2M=4$	
2	0.83	0.89	0.013
4	0.83	0.85	0.015
8	0.83	0.84	0.018
16	0.83	0.87	0.018
32	0.83	0.92	0.012
		$2M=6$	
2	1.0	0.84	0.0080
4	1.0	0.82	0.0080
8	1.0	0.81	0.0082
16	1.0	0.85	0.0101
32	1.0	0.90	0.0089
		$2M=8$	
2	1.15	0.87	0.0012
4	1.15	0.85	0.0016
8	1.15	0.83	0.0043
16	1.15	0.85	0.0062
32	1.15	0.89	0.0063

proceeds. On the other hand, as the model of Fig. 4 can be calculated exactly, we shall use the comparison between the exact and the approximate solution for analyzing the validity of our approximations and, in particular, of the correlation energy given by Eq. (74).

In a second step we consider a more realistic quantum dot model where the electron reservoirs have a continuous density of states. Finally, we apply our approach to a multiband Hubbard lattice.

A. Multilevel Anderson model

1. Zero band-width limit 2M=4

In this calculation, we present results for a nondegenerate case with $2M=4$ ($\varepsilon_1 \neq \varepsilon_2$). The reservoirs are simulated by sharp levels (Fig. 4).

Figure 6(a) shows n_1 and n_2 as a function of the ''Fermi energy'' (in this model, this is the energy of the sharp levels simulating the reservoirs), for $\tilde{U}/T=4$, 8, 10, and 16, and $\varepsilon_1-\varepsilon_2=T$. Exact results are given in full lines, the results of our approach are given in short-dashed lines, and the HF results are given in long-dashed lines. Comparison between exact and approximate results shows that our method yields reasonable values of n_1 and n_2 up to $\tilde{U}/T\approx 10$. For smaller values, say $\tilde{U}/T\approx 4$, our approximation is excellent, representing a substantial improvement upon the HF solution. We should comment that for $\tilde{U}/T\approx 16$, our solution is also very good except in a small region of energy for which $n_1+n_2 \simeq 1$; even in this case, our solution is reasonable.

Figure 6(b) shows similar results for $\varepsilon_1-\varepsilon_2=2T$. The exact solution of this case is even better reproduced by our solution than the previous one, with n_1 and n_2 very well approximated even for $\tilde{U}/T=16$. We conclude that the case $\varepsilon_1-\varepsilon_2=T$ corresponds to the most unfavorable case (for $\varepsilon_1=\varepsilon_2$, our results reproduce very well the exact solution), and shows that we can use with great confidence the approximations presented in the previous section up to values of $\tilde{U}/T\approx 10$.

2. Quantum dots (2M=4)

As a more realistic model for a multilevel quantum dot or an Anderson impurity, we consider the generalized Anderson model given by $H=H_0+H_{\rm res}+H_T$, where $H_0=\Sigma_m \epsilon_m \hat{d}_m^\dagger \hat{d}_m + U\Sigma_{l>m}\hat{n}_m\hat{n}_l$ corresponds to the uncoupled QD ($\hat{n}_m=\hat{d}_m^\dagger\hat{d}_m$); $H_{\rm res}=\Sigma_k \epsilon_k \hat{c}_k^\dagger \hat{c}_k$ to the uncoupled reservoir, and $H_T=\Sigma_{m,k} t_{m,k}\hat{d}_m^\dagger \hat{c}_k + \text{H.c.}$ describes the coupling between the dot and the reservoirs. The labels m and l ($0 \leqslant m,l \leqslant 2M$) in H denote the different dot levels including spin quantum numbers. We adopt the usual simplifying assumption of having the same electron-electron interaction U between any pair of dot states.

When applying the formalism of Sec. III for the present model we assume that the tunneling rate, given by $i\Delta_m=\Sigma_k t_{m,k}^2/(\omega-\epsilon_k+i0^+)$, is independent of the energy. With this assumption the effective densities of states ρ_i become simple Lorentzian functions.

As in the case of sharp levels we have studied the $2M=4$ case for different values of U/Δ_m. Figures 7(a) and 7(b) show the charge per dot level as a function of the leads Fermi energy, for $U/\Delta_m=13.3$ and 8, as calculated using either our LD potential or the self-energy approach. We also show, for comparison, the Hartree-Fock solution. For the LD calculation, we need to calculate the mean excitation energy W_α associated with each orbital, in order to use Eq. (75). We have found, using Eqs. (64) and (65), that for $0.1 \leqslant n_{i\alpha} \leqslant 0.9$, it is a good approximation to write

$$W_\alpha = 2.52\Delta_m \left[1.25 + \tan^2 \pi \left(n_{i\alpha\sigma} - \frac{1}{2} \right) \right]^{1/2}. \qquad (76)$$

The comparison of the different solutions presented in Figs. 7(a) and 7(b) shows that our LD calculation and our self-energy solution yield very similar charges mainly in the region $U/\Delta_m \leqslant 10$, where we can take our solutions with great confidence (in this case, Δ plays approximately the role of T in the zero bandwidth limit). In Fig. 7, we can also see that our correlated solutions present a substantial improvement over the HF one.

It is interesting to comment how our self-energy solution can be used to calculate the quasiparticle spectral densities. This property depends strongly on the charge within the dot. Figure 8 illustrates the evolution of the interacting densities of states when increasing the charge inside the dot for the fully degenerate case ($\epsilon_1=\epsilon_2$). One can observe that for $n \ll 1.0$ the DOS consists of a broad quasi-Lorentzian resonance centered slightly above the Fermi energy. This behavior corresponds to the so-called mixed valence regime.[41] When $n \geqslant 1$ the system is in the Kondo regime and the DOS

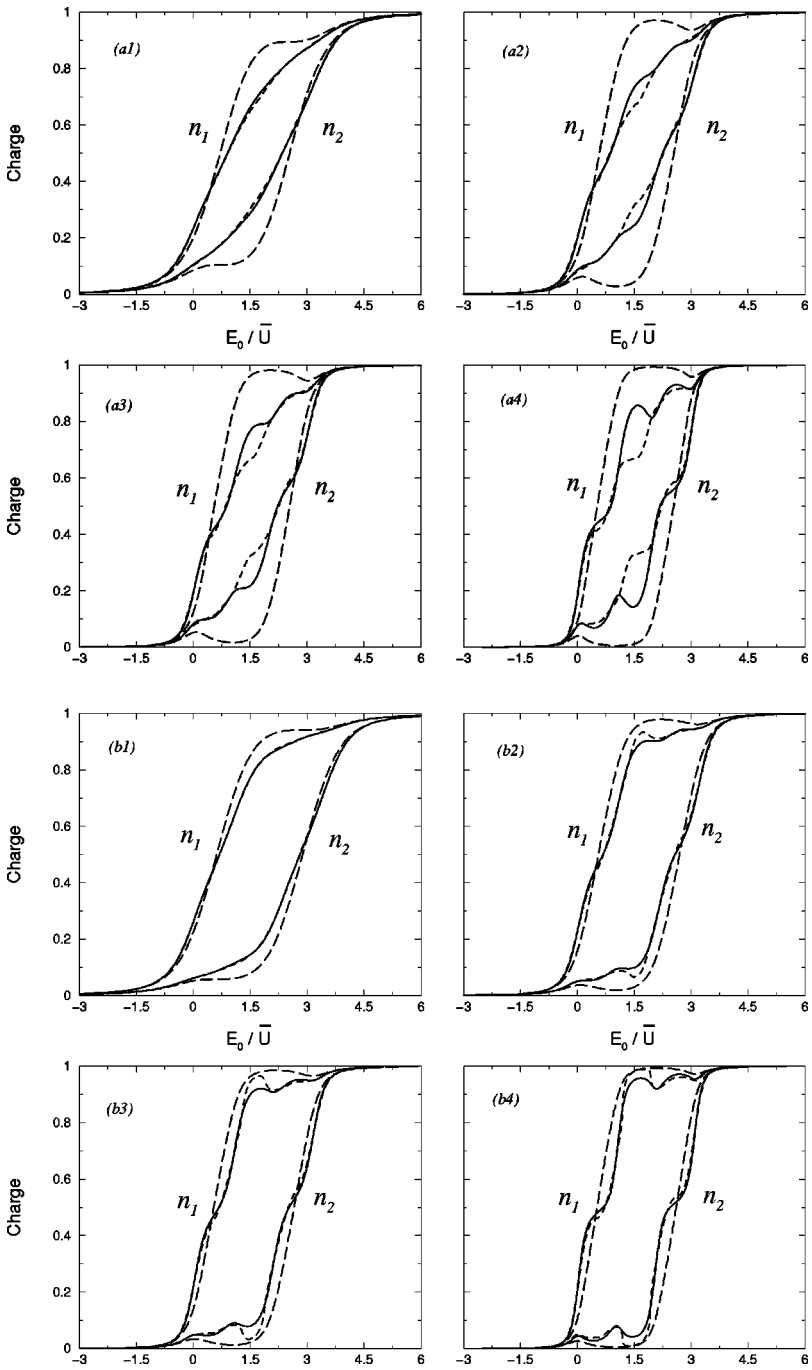

FIG. 6. (a) Occupancies $n_{1\sigma}$ and $n_{2\sigma}$, for the atomic model of Fig. 4 with $2M=4$, as a function of the ''reservoirs'' level $E_0/\tilde{U}$, for $E_1=0$, $E_2=T$ and different $\tilde{U}/T$ values. (a) The first set of four figures (labeled a1–a4) corresponds to the case $E_1=0$, $E_2=T$, and $\tilde{U}/T=4$, 8, 10, and 16. (b) Same as (a), for $E_1=0$ and $E_2=2T$. Full lines: exact solution. Short dashed lines: our solution using Eq. (72). Long dashed lines: HF solution.

exhibits a narrow resonance around the Fermi energy and two broader resonances at the charge excitation energies ϵ and $\epsilon+U$. These two resonances are in general not symmetric except for the half-filled case $n\sim 2$, due to the hole-electron symmetry.[28]

B. Multiband Hubbard lattice: $2M=2$ and 4

In this section we consider the case of a multiband Hubbard lattice, with the following Hamiltonian:

$$\hat{H}=-T\sum_{i,j(\mathrm{NN})}\hat{c}^{\dagger}_{i\alpha\sigma}\hat{c}_{j\alpha\sigma}+\frac{1}{2}\sum_{\alpha\sigma\neq\beta\sigma'}U_i\hat{n}_{i\alpha\sigma}\hat{n}_{i\beta\sigma'} \quad (77)$$

and analyze two cases, with either a singly or doubly degenerate level per site. In Eq. (77), we also assume the atoms to form a square lattice with each atom having four nearest neighbors. The case of a simply degenerate level with one electron per site has been discussed elsewhere.[24,43] Here, for the sake of completeness we only show in Fig. 9 the evolution of its local DOS as a function of U/T. This is a case that has been analyzed using the many-body techniques discussed above. For sake of simplicity we have replaced the square lattice by a Bethe lattice with coordination 4. As Fig. 9 shows, the DOS of this system evolves presenting a narrower band around E_F for larger U/T values; eventually, a Hubbard-Mott transition is found for $U/T\gtrsim 13$. It is worth commenting that this metal-insulator transition has been calculated using the local-self-energy described in Sec. III, complemented with the consistent description introduced by Georges *et al.*[24] for infinite dimension, within the DMF approximation.

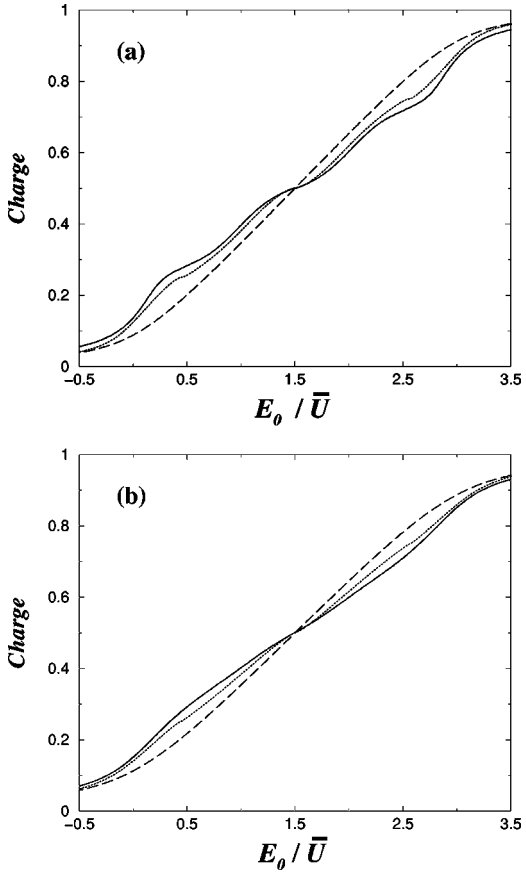

FIG. 7. (a) Occupancy n_i, as a function of the reservoirs level, for the quantum dot model discussed in the text. ($2U/\Delta = 13.3$). Full line: self-energy solution. Short-dotted line: LD solution. Long-dashed line: HF solution. (b) As (a), for $2U/\Delta = 8$.

As a second example we analyze the case of a doubly degenerate level per site, with a quarter filling (1 electron per site). This is a case that has received recently some attention as a model of a magnetic material.[40] For studying this case, including its band structure and the possible Hubbard-Mott transition, we use the many-body techniques discussed above, neglecting off-diagonal self-energies.

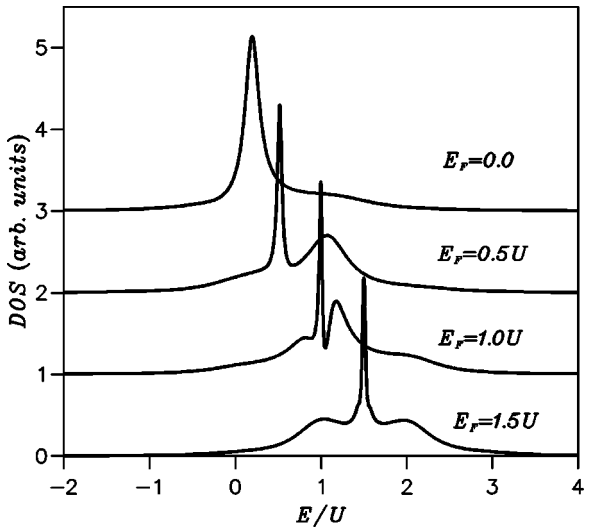

FIG. 8. DOS as a function of the reservoir level for the same model analyzed in Fig. 7(b) ($2U/\Delta = 8$).

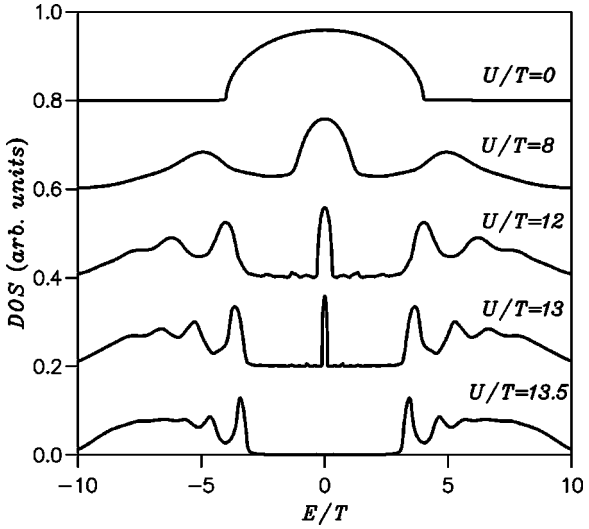

FIG. 9. DOS for the two-dimensional Hubbard model discussed in the text. Here, we consider a singly half occupied degenerate level and different U/T values. The Fermi level is taken as the origin of energies.

Figure 10 shows the evolution of the local DOS for increasing values of U/T (as in the previous case, we use a Bethe lattice replacing the actual one). For this case, the ground state is obtained by looking for a ferromagnetic solution, with different occupancies for spins up or down. (One should notice that for this particular model the ferromagnetic solution is degenerate in energy with a nonmagnetic solution having charge transfer between the two levels in each site. Differences between these solutions can only be obtained if a more complete Mott-Hubbard model in introduced including Hund rules.) In Fig. 10 we also show the occupancies of the two different spin occupancies. For $U/T \lesssim 13$, the system appears to be paramagnetic with a band structure that gets narrower around E_F for larger U/T values, while, at the same time, two main peaks appear above and below E_F. For U/T

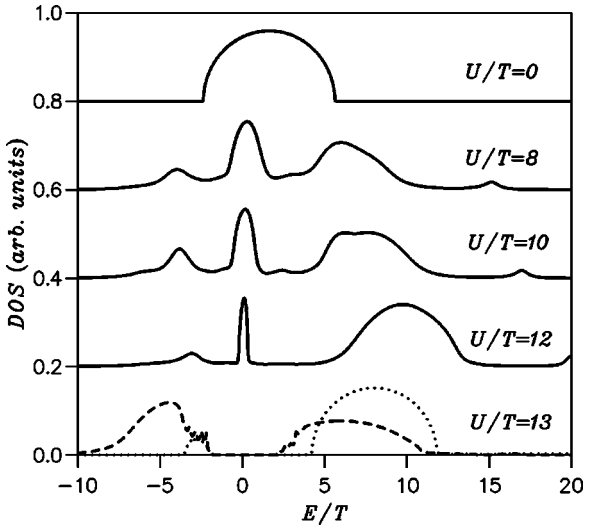

FIG. 10. DOS for a Hubbard model, where we have a doubly quarter-filled degenerate level and different U/T values. For $U/T = 13$, we show the DOS for both spins. For $U/T \leqslant 12$, the solution is paramagnetic. The Fermi level is taken as the origin of energies.

close to $U/T \simeq 13$, the band DOS evolves into a Kondo like peak and, eventually, for U/T larger than 13 the system appears to be semiconducting, and behaves as a ferromagnetic system. It is interesting to compare this solution with the one found for the singly degenerate level: in both cases, the metal-insulator transition appears for $U/T \simeq 13$. This shows that the solution of the doubly degenerate level can be understood in terms of the simply degenerate case: as soon as U/T is large enough for yielding an insulator in the $2M=2$ case, the second level is repelled to higher energies and the system becomes ferromagnetic. (We should comment that in our solution for $2M=4$, the two states with the occupied spins become equivalent to the singly degenerate case of the model discussed above.)

These results can be checked by comparing with recent calculations by Homoi *et al.*[40] who analyzed the same structure with different band-filling factors. In the half-filled case, those authors have found the Mott-Hubbard transition for $U/W=3$, where W is the band-width of the initial DOS (in our case, $W=4T$), in agreement with our results.

V. DISCUSSION: HOW TO APPLY PREVIOUS RESULTS TO CRYSTALS AND MOLECULES

In the previous sections we have shown how to introduce, within the local density dynamical mean field approximation, the exchange-correlation potential associated with a generalized Hubbard Hamiltonian. Models based on this Hamiltonian are often used for analyzing the electronic properties of highly correlated systems. Although they provide a good qualitative description, new terms have to be included in the Hamiltonian in order to get a satisfactory quantitative description of realistic systems such as molecules or solids. In this section, we discuss these new many-body terms and show how this more complex Hamiltonian can be solved using the ideas discussed above. In particular, we compare the results obtained by this method with standard approaches such as DFT-LDA or GGA calculations in solid state theory, and configuration interaction (CI) in quantum chemistry. The discussion concerning small molecules is particularly relevant, because it illustrates how to go beyond the dynamical mean field approximation.

A. Bulk solids

We write the general Hamiltonian for the crystal electrons as follows:

$$\hat{\mathcal{H}}=\sum_{\nu,\sigma}(\epsilon_\nu+V^{\rm ps}_{\nu\nu,\sigma})\hat{n}_{\nu,\sigma}+\sum_{\mu\neq\nu,\sigma}(t_{\mu\nu,\sigma}+V^{\rm ps}_{\mu\nu,\sigma})\hat{c}^\dagger_{\mu\sigma}\hat{c}_{\nu\sigma}+\frac{1}{2}\sum_{\nu\omega\sigma\mu\lambda\sigma'}O^{\nu\mu}_{\omega\lambda}\hat{c}^\dagger_{\nu\sigma}\hat{c}^\dagger_{\mu\sigma'}\hat{c}_{\lambda\sigma'}\hat{c}_{\omega\sigma}, \tag{78}$$

where $\nu\equiv i,\alpha$ and

$$\epsilon_\nu=\int\varphi_\nu(\overline{r})\left(-\frac{\nabla^2}{2}-\sum_\alpha\frac{Z_\alpha}{|\overline{r}-\overline{R}_\alpha|}\right)\varphi_\nu(\overline{r})d\overline{r},$$

$$t_{\nu\mu}=\int\varphi_\nu(\overline{r})\left(-\frac{\nabla^2}{2}-\sum_\alpha\frac{Z_\alpha}{|\overline{r}-\overline{R}_\alpha|}\right)\varphi_\mu(\overline{r})d\overline{r}, \tag{79}$$

$$O^{\nu\mu}_{\omega\lambda}=\int\varphi_\nu(\overline{r})\varphi_\omega(\overline{r})\frac{1}{|\overline{r}-\overline{r}'|}\varphi_\mu(\overline{r}')\varphi_\lambda(\overline{r}')d\overline{r}d\overline{r}'.$$

$V^{\rm ps}_{\mu\nu,\sigma}$ are the matrix elements of the pseudopotential.[22] The sums in $\nu,\mu,\ldots$, extend only to the valence orbitals in each site i.

The many-body terms of Hamiltonian (78) include different types of contributions, among them the Coulomb interactions U_ν and $J_{\nu\mu}$ appearing in the generalized Hubbard Hamiltonian discussed above, and hybrid interactions as $h\hat{n}\hat{c}^\dagger\hat{c}$. In all these contributions only three different orbitals are involved at most. We can separate these terms and write the many-body contribution as follows:

$$\begin{aligned}\frac{1}{2}\sum_{\nu\omega\sigma\mu\lambda\sigma'}O^{\nu\mu}_{\omega\lambda}\hat{c}^\dagger_{\nu\sigma}\hat{c}^\dagger_{\mu\sigma'}\hat{c}_{\lambda\sigma'}\hat{c}_{\omega\sigma}&=\sum_\nu U_\nu\hat{n}_{\nu\uparrow}\hat{n}_{\nu\downarrow}\\&+\frac{1}{2}\sum_{\mu\neq\nu,\sigma\sigma'}J_{\nu\mu}\hat{n}_{\nu\sigma}\hat{n}_{\mu\sigma'}\\&+\sum_{\mu\neq\nu,\lambda,\sigma\sigma'}h_{\lambda,\nu\mu}\hat{n}_{\lambda\sigma'}\hat{c}^\dagger_{\nu\sigma}\hat{c}_{\mu\sigma}\\&-\sum_{\mu\neq\nu,\lambda,\sigma}h^x_{\lambda,\nu\mu}\hat{n}_{\lambda\sigma}\hat{c}^\dagger_{\nu\sigma}\hat{c}_{\mu\sigma}+\frac{1}{2}\sum_{N.N.}O^{\nu\mu}_{\omega\lambda}(\hat{c}^\dagger_{\nu\sigma}\hat{c}_{\omega\sigma})\\&\times(\hat{c}^\dagger_{\mu\sigma'}\hat{c}_{\lambda\sigma'})+\text{other terms},\end{aligned} \tag{80}$$

where U_ν, $J_{\nu\mu}$, $h_{\lambda,\nu\mu}$, and $h^x_{\lambda,\nu\mu}$ are defined by

$$h_{\lambda,\nu\mu}=\int\varphi^2_\lambda(\overline{r})\frac{1}{|\overline{r}-\overline{r}'|}\varphi_\nu(\overline{r}')\varphi_\mu(\overline{r}')d\overline{r}d\overline{r}', \tag{81}$$

$$h^x_{\lambda,\nu\mu}=\int\varphi_\lambda(\overline{r})\varphi_\nu(\overline{r})\frac{1}{|\overline{r}-\overline{r}'|}\varphi_\lambda(\overline{r}')\varphi_\mu(\overline{r}')d\overline{r}d\overline{r}', \tag{82}$$

$$U_\nu=\int\varphi^2_\nu(\overline{r})\frac{1}{|\overline{r}-\overline{r}'|}\varphi^2_\nu(\overline{r}')d\overline{r}d\overline{r}', \tag{83}$$

$$J_{\nu\mu}=\int\varphi^2_\nu(\overline{r})\frac{1}{|\overline{r}-\overline{r}'|}\varphi^2_\mu(\overline{r}')d\overline{r}d\overline{r}'. \tag{84}$$

Notice that among all the remaining contributions $O^{\nu\mu}_{\omega\lambda}$ we have singled out those where ν,μ,ω, and λ belong either to one atom or to nearest-neighbor atoms (indicated by $\Sigma_{\rm NN}$). These are the terms which have to be retained in order to get a good description of the energy of the system. The most important contributions in $\Sigma_{\rm NN}$ come from the dipole-dipole interaction given by the terms where $\nu\neq\omega\in i,\mu\neq\lambda\in j,\sigma\sigma'$, and from the exchange interaction $-\frac{1}{2}\Sigma_{\mu\neq\nu}J^x_{\nu\mu}\hat{n}_{\nu\sigma}\hat{n}_{\mu\sigma}$, where

$$J^x_{\nu\mu}=\int\varphi_\nu(\overline{r})\varphi_\mu(\overline{r})\frac{1}{|\overline{r}-\overline{r}'|}\varphi_\nu(\overline{r}')\varphi_\mu(\overline{r}')d\overline{r}d\overline{r}'. \tag{85}$$

We have found that the rest of the terms [labeled *other terms* in Eq. (80)] give a very small contribution to the total

energy of the system and are going to be neglected. We call this approximation the LCAO-OO (orbital occupancy) approximation.

The resulting LCAO-OO Hamiltonian reads as follows:

$$\hat{\mathcal{H}}_0=\sum_{\nu\sigma}(\epsilon_\nu+V^{\rm ps}_{\nu\nu,\sigma})\hat{n}_{\nu\sigma}+\sum_{\nu\neq\mu,\sigma}\hat{T}_{\nu\mu,\sigma}\hat{c}^\dagger_{\nu\sigma}\hat{c}_{\mu\sigma}+\sum_\nu U_\nu\hat{n}_{\nu\uparrow}\hat{n}_{\nu\downarrow}+\frac{1}{2}\sum_{\nu\neq\mu,\sigma,\sigma'}J_{\nu\mu}\hat{n}_{\nu\sigma}\hat{n}_{\mu\sigma'}+\frac{1}{2}\sum_{n.n.}O^{\nu\mu}_{\omega\lambda}(\hat{c}^\dagger_{\nu\sigma}\hat{c}_{\omega\sigma})(\hat{c}^\dagger_{\mu\sigma'}\hat{c}_{\lambda\sigma'}),\tag{86}$$

where the *hopping* term $\hat{T}_{\nu\mu,\sigma}$ is defined by

$$\hat{T}_{\nu\mu,\sigma}=\left[t_{\nu\mu}+V^{\rm ps}_{\nu\mu,\sigma}+\sum_{\lambda,\sigma'}h_{\lambda,\nu\mu}\hat{n}_{\lambda\sigma'}-\sum_\lambda h^x_{\lambda,\nu\mu}\hat{n}_{\lambda\sigma}\right].\tag{87}$$

We can now make contact with the generalized Hubbard Hamiltonians discussed in the previous sections introducing the Hamiltonian $\hat{\tilde{\mathcal{H}}}_0$:

$$\hat{\tilde{\mathcal{H}}}_0=\sum_{\nu\sigma}(\epsilon_\nu+V^{ps}_{\nu\nu,\sigma})\hat{n}_{\nu\sigma}+\sum_{\nu\neq\mu,\sigma}T_{\nu\mu,\sigma}\hat{c}^\dagger_{\nu\sigma}\hat{c}_{\mu\sigma}+\sum_\nu U_\nu\hat{n}_{\nu\uparrow}\hat{n}_{\nu\downarrow}+\frac{1}{2}\sum_{\nu\neq\mu,}J_{\nu\mu}\hat{n}_\nu\hat{n}_\mu,\tag{88}$$

where $T_{\nu\mu,\sigma}$ is given by Eq. (87), replacing $\hat{n}_{\lambda\sigma}$ by the occupation number $n_{\lambda\sigma}$. This Hamiltonian $\hat{\tilde{\mathcal{H}}}_0$ is now completely analogous to the generalized Hubbard Hamiltonians we have considered so far and can be treated using the techniques described in Secs. II and III. For the difference between $\hat{\mathcal{H}}_0$ and $\hat{\tilde{\mathcal{H}}}_0$, $\delta\hat{\tilde{\mathcal{H}}}_0$, we propose to use a Hartree-Fock approximation. Thus, the total energy E_0 of Hamiltonian (86) is calculated as the sum of $\tilde{E}_0$, the ground-state energy of Eq. (88), and the Hartree-Fock (HF) mean value of $\delta\hat{\tilde{\mathcal{H}}}_0$:

$$\langle\delta\hat{\tilde{\mathcal{H}}}_0\rangle_{\rm HF}=-\sum_{\nu\neq\mu,\sigma}\left[\sum_\lambda(h_{\lambda,\nu\mu}-h^x_{\lambda,\nu\mu})n_{\nu\lambda\sigma}n_{\mu\lambda\sigma}\right]+\frac{1}{2}\sum_{\rm NN,\sigma}O^{\nu\mu}_{\omega\lambda}(n_{\mu\lambda\sigma}n_{\nu\omega\sigma}-n_{\nu\lambda\sigma}n_{\mu\omega\sigma}).\tag{89}$$

Regarding the solution of Hamiltonian (88), it has to be noticed that the intra-atomic Coulomb interaction within a site i, say $U_\nu\equiv U_{i\alpha}$ and $J_{\nu\mu}\equiv J_{i\alpha,i\beta}$, are different from each other, at variance with the generalized Hubbard Hamiltonian (1) that we have considered so far, where it was assumed $U_{i\alpha}=J_{i\alpha,i\beta}=U_i$. In problems where an atomic minimal basis is used, one finds that the differences between those intraatomic interactions are small. In these cases, it is well justified to calculate the intraatomic correlation energy E^I with Eq. (75), using for each orbital $i\alpha$ a different Coulomb interaction $\tilde{U}_{i\alpha}$ defined by $(U_{i\alpha}-J^{\rm NN}_{i\alpha})$.

We have checked the accuracy of this approach considering the case of bulk Si. We have used a LCAO-OO Hamiltonian with an optimized sp^3 minimal basis. Details of the implementation of the method and the use of a extended basis (including *d* orbitals) will be published elsewhere. Here we focus on the comparison of our method with another localized orbital scheme such as FIREBALL96,[17] where a minimal sp^3 basis is also used, and standard LDA and GGA plane wave implementations. The FIREBALL96 calculation uses contracted atomic orbitals generated with a cutoff radius $R_c=5$ a.u.[13]

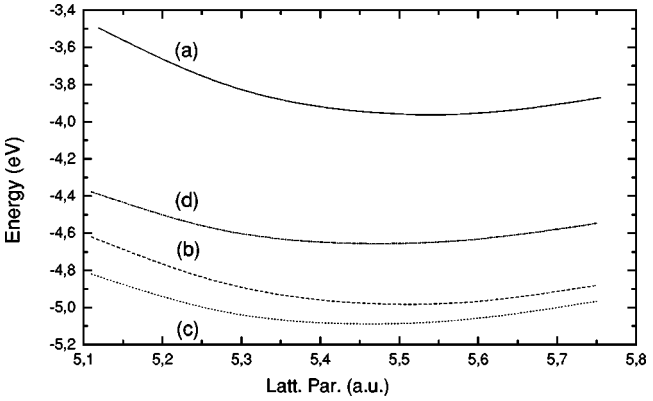

FIG. 11. Cohesive energy of Si as a function of the lattice parameter for (a) full line, our LCAO-OO model; (b) long-dashed line, FIREBALL; (c) short-dashed line, LDA; and (d) dotted-dashed line, GGA.

Figures 11 and 12 show the results obtained with the different methods for the total energy per atom (cohesive energy) and the exchange-correlation (XC) energy per atom as a function of the lattice parameter. In all the cases we are taking as a reference for the total energy or the exchange-correlation energy the value calculated for the isolated atom with the corresponding method. Notice that in the case of FIREBALL and the DFT-PW calculations we have to include a correction for the spin-polarization energy in the calculation of the total energy for the isolated atom. We have taken a value of -0.65 eV, according to Ref. 42. In order to make the comparison between our method and the other approaches meaningful we have to include in the LCAO-OO Hartree energy the electrostatic self-interaction energy associated with each orbital occupancy, a term that is automatically not included in our approach. Table II compares the total energy and XC energy calculated with different methods for the experimental lattice constant 5.43 Å. The well known overestimation of the cohesive energy by all the

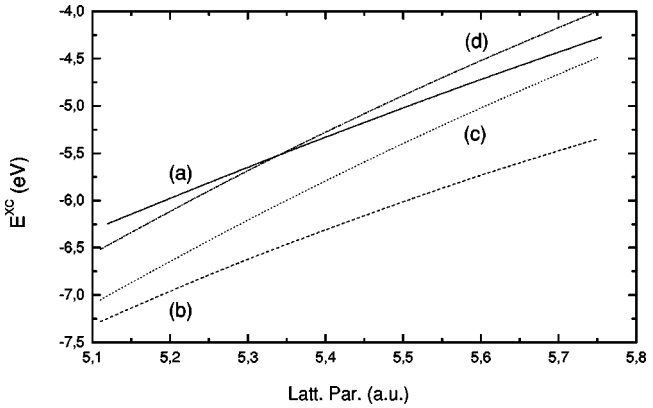

FIG. 12. As in Fig. 11 for the exchange-correlation energy.

TABLE II. Cohesive energy ($E_{\rm tot}$) and exchange-correlation energy ($E_{\rm XC}$), both in eV, for bulk Si calculated with different methods for the experimental lattice constant.

	LCAO-OO	FB	LDA	GGA	Exp.
$E_{\rm tot}$	3.95	5.00	5.10	4.65	4.60
$E_{\rm XC}$	5.23	6.15	5.60	5.10	

methods based in LDA is clearly shown. GGA considerably improves the result of LDA calculations. The LCAO-OO method is the only one providing an upper bound to the cohesive energy. This is related to the better description of the XC energy (see below) and to the fact that both our LCAO-OO and the FIREBALL96 calculations use a minimal basis: more complete basis will be needed in order to get a converged value of the Hartree and kinetic energy contributions.

A fairer estimation of the relative merit of the different methods in the description of the exchange and correlation would therefore be provided by a direct comparison of the XC energy. We assume that the Hartree and kinetic energies are well converged in the DFT calculations (both LDA and GGA) with a plane wave basis. Using these values and the experimental Si cohesive energy we can determine that the value of the XC energy, at the experimental lattice parameter, should be 5.10 eV. Our LCAO-OO approach is within an error of only 0.1 eV when compared with that value, while all the LDA based methods significantly overestimate the XC energy. The GGA approximation improves over the LDA results, providing a value close to our LCAO-OO method. Notice that the overestimation of the XC energy in FIREBALL96, larger than the LDA-PW case, is mainly due to a further approximation used for the fast evaluation of the exchange-correlation matrix elements (see Sec. IV D in Ref. 13). When this approximation is improved (using the method proposed in Ref. 21) the XC energy comes closer to the LDA-PW result.

We conclude from this analysis that our LCAO-OO approach, using the formalism discussed above, seems to provide a very good description, comparable to the GGA approximation, of the exchange-correlation energies in the limit of low correlation, as shown in the case of bulk Si. Our method combines a significant improvement over the LDA approach for this low correlation limit with the ability to describe the high correlation limit tested in Sec. IV.

B. Small molecules

The second example we address in this section is the case of molecules. Our basic approach to this system is similar to the one discussed above for crystals. We take as the starting point the same LCAO-OO Hamiltonian $\hat{\mathcal{H}}_0$ [Eq. (86)], which we also reduce to the generalized Hubbard Hamiltonian [Eq. (88)]. As in the case of crystals, we approximate the ground-state energy of Eq. (86) E_o by the one associated with Hamiltonian [Eq. (88)], $\tilde{E}_o$, plus the contribution $\langle \delta\hat{\tilde{\mathcal{H}}}_0\rangle_{\rm HF}$, in similarity with Eq. (89).

The analysis of Hamiltonian (88) for molecules has to be changed, however, with respect to our previous discussion for the following reasons. First of all, we have to realize that

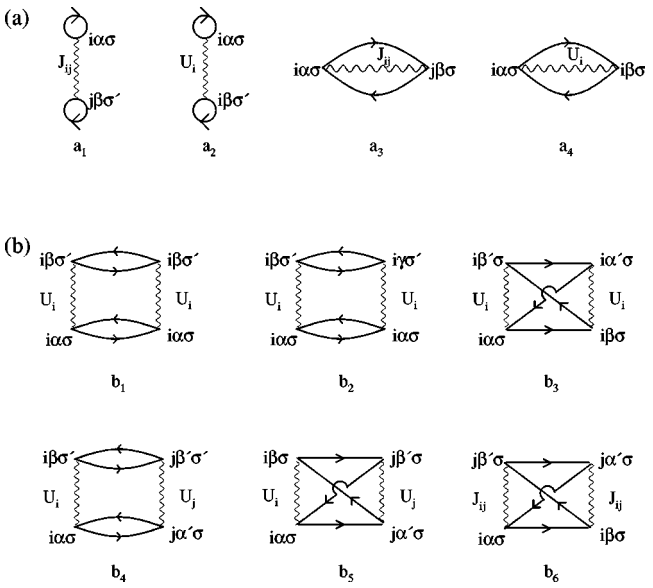

FIG. 13. First and second order perturbative diagrams contributing to the total energy of the Hubbard Hamiltonian. Only a few second order diagrams are shown.

the condition $n_{i\alpha\sigma;i\beta\sigma}=0$ is not satisfied due to the reduced symmetry in the molecule. Recalling the results in Sec. II B, this implies that the exchange hole $(1-n_{i\alpha\sigma})$ is not completely located beyond the local site *i*. A fraction of this hole is also located inside the atom *i*, increasing the effective interaction, $J_{i\alpha\sigma}$, between $n_{i\alpha\sigma}$ and its hole $(1-n_{i\alpha\sigma})$, due to the larger intra-atomic coulomb interaction.

We analyze this case introducing a factor $x(n_{i\alpha\sigma})$ that takes into account the hole fraction located inside the site *i*, a value that can be calculated from the density matrix $n_{ij\sigma}(\omega)$ [see Eq. (12)]. Thus, we write the exchange and extra-atomic correlation energy as follows:

$$\tilde{E}^{\rm XC}[\{n_{i\alpha\sigma}\}]=-\frac{1}{2}\sum_{i\alpha\sigma} J_{i\alpha}n_{i\alpha\sigma}(1-n_{i\alpha\sigma}), \qquad (90)$$

where

$$J_{i\alpha}=(1-x_{i\alpha})J_{i\alpha}^{\rm NN}+x_{i\alpha}U_i, \qquad (91)$$

and U_i is the mean Coulomb interaction in the site *i*. In our approach, Eq. (90) replaces Eq. (20) for $x_{i\alpha}$ different from zero (in other words, for $n_{i\alpha\sigma;i\beta\sigma}\neq 0$). Notice that for the sake of clarity we have assumed $x_{i\alpha}$ and thus $J_{i\alpha}$ to be spin independent, but the formalism can be extended in a straightforward manner to the case of spin polarization.

On the other hand, we have to change also our treatment of the intraatomic correlation energy $E^I[\{n_{i\alpha\sigma}\}]$ for Hamiltonian (88). It is convenient to discuss this point by considering first the DMF approximation discussed above from a different perspective. To this end, consider the first and second order Feynman diagrams (shown in Fig. 13) contributing to the energy of the system. In the DMF approach the first order exchange diagram (a_3 in Fig. 13) yields Eq. (20), since the exchange hole is located in the nearest-neighbor sites (remember that we assumed $n_{i\alpha\sigma;i\beta\sigma}=0$). Now, we consider the second order diagrams. In our approach so far we did this introducing the reduced Hamiltonian (25). The important

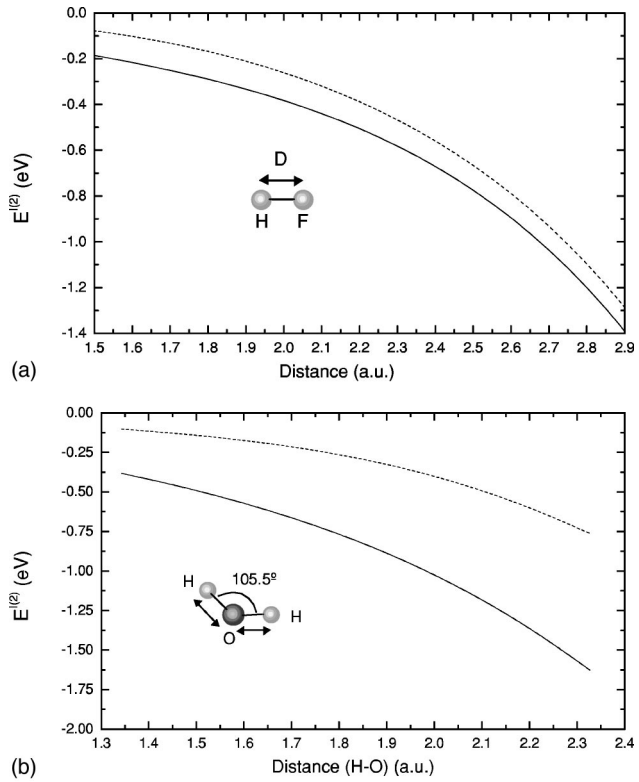

FIG. 14. (a) Second order correlation energy for HF: full line, diagonal term; dashed line, off-diagonal term. (b) Same for H_2O. Calculations are performed using an optimized minimal basis: HF: $H(1s)F(1s^2,2s^2,2p^2)$;H_2O:$H(1s)O(1s^2,2s^2,2p^2)$.

point to notice is that the introduction of the reduced Hamiltonian (25) is equivalent to the replacement of the different U and J interactions by the screened values given by

$$\tilde{U}_i = U_i - J_i^{\mathrm{NN}}, \tag{92}$$

$$\tilde{J}_{ij} = 0.$$

This is physically very reasonable, because in a lattice with infinite dimensions, the interaction between charges located at different sites are screened out completely by the charge induced in the nearest-neighbor sites. Moreover, charges located in the same atom see also the screened charge cloud that reduces U to $\tilde{U}_i = U_i - J_i^{\mathrm{NN}}$, with J_i^{NN} being the interaction between an electron located in the atom and that charge cloud.

With the new effective interactions $\tilde{U}_i$ and $\tilde{J}_{ij}$ we find that only the diagrams with $\tilde{U}_i^2$ or $\tilde{U}_i\tilde{U}_j$ contribute to the second order energy. We should also realize that in the DMF approximation all the interatomic off-diagonal terms $n_{i\alpha\sigma;j\beta\sigma}$ can be neglected (remember that we have assumed that $n_{i\alpha\sigma;i\beta\sigma}=0$ inside the atom). This shows that, in a second order perturbation theory, only the diagram labeled b_1 in Fig. 13 contributes to the energy. This is precisely what we considered in Sec. III as part of the argument leading to $E^I[\{n_{i\alpha\sigma}\}]$.

Coming back to the case of molecules, we have found that in the exchange-extraatomic correlation energy $J_{i\alpha}^{\mathrm{NN}}$ is changed by $J_{i\alpha}$ [Eq. (91)]. This is equivalent to introducing the diagram a_4 in Fig. 13. In analogy with the DMF, this result suggests to introduce screened values of the interactions that we define for the new case as follows:

$$\tilde{U}_{i\alpha} = U_{i\alpha} - J_{i\alpha}, \tag{93}$$

$$\tilde{J}_{ij} = 0.$$

We also reach the same conclusion, considering how the total exchange-correlation energy appears as a modification of the initial hole $(1-n_{i\alpha\sigma})$, that is partially changed into a new correlation hole $f_{i\alpha\sigma}(1-n_{i\alpha\sigma})$. This can be understood more clearly if we write [following Eq. (23)]:

$$E^{\mathrm{XC}}[\{n_{i\alpha\sigma}\}] = -\frac{1}{2}\sum_{i\alpha\sigma}\Big[(1-f_{i\alpha\sigma})J_{i\alpha}n_{i\alpha\sigma}(1-n_{i\alpha\sigma}) - \frac{1}{2}\sum_{i\alpha\sigma} f_{i\alpha\sigma}U_{i\alpha}n_{i\alpha\sigma}(1-n_{i\alpha\sigma}) \tag{94}$$

with $f_{i\alpha\sigma}$ representing the new correlation hole fraction inside the site i. Equation (94) shows that $(U_{i\alpha}-J_{i\alpha})$ is the effective interaction associated with the correlation fluctuations created by the intrasite Coulomb potential, in agreement with Eq. (93). This result suggests to calculate the correlation energy associated with the intra-atomic fluctuations using the screened interactions $\tilde{U}_{i\alpha}=U_{i\alpha}-J_{i\alpha}$ and $\tilde{J}_{ij}=0$. In the DMF approximation, this energy is calculated in second order perturbation theory using only the diagram b_1 in Fig. 13. In the case of systems for which $n_{i\alpha\sigma;j\beta\sigma}\neq 0$ and $n_{i\alpha\sigma;i\beta\sigma}\neq 0$ we also have to include other diagrams, similar to the ones shown in Fig. 13, which are proportional to $\tilde{U}_i^2$ or $\tilde{U}_i\tilde{U}_j$. Consider first the diagrams labeled b_1, b_2 and b_3, which are proportional to $\tilde{U}_i^2$. One can prove easily, using the sum rule [Eq. (10)], that when we move from diagrams b_1 to b_2 and b_3, the contribution of these second order terms to $E^{I(2)}$ decreases in every step faster than the fraction of hole $x_{i\alpha\sigma}$ [see Eq. (91)] that becomes localized in the atom i. Typically one finds that the diagram b_2 contributes roughly as $x_{i\alpha\sigma}/2$ times the diagram b_1. Similarly, diagram b_3 contributes like $x_{i\alpha\sigma}/2$ times the diagram b_2. On the other hand, we have found in typical cases (see below) that $x_{i\alpha\sigma}$ is never larger than 0.2–0.3. Then, we conclude that one can neglect the diagrams b_2 and b_3 with an accuracy better than 15% in the calculation of $E^{I(2)}$.

Consider next diagrams b_4 and b_5. We also find that diagram b_5 is negligible compared with b_4. However, we have found that diagram b_4 can be important and ,in some cases, comparable to the contribution given by b_1 (see the discussion below).

This means that in second order perturbation theory, we can calculate $E^{I(2)}$ using only diagrams b_1 and b_4. Thus, we should replace Eq. (65) by the following expression:

$$E^{I(2)}[\{n_{i\alpha\sigma}\}] = -\sum_i \left\{ \frac{\tilde{U}_i^2}{2} \sum_{\alpha\sigma\neq\beta\sigma'} \frac{n_{i\alpha\sigma}(1-n_{i\alpha\sigma})n_{i\beta\sigma'}(1-n_{i\beta\sigma'})}{W_{\alpha\beta}} - \sum_{j(\neq i)} \frac{\tilde{U}_i\tilde{U}_j}{2} \sum_{\alpha'\sigma'(\neq\alpha\sigma),\beta\sigma\neq\beta'\sigma'} \times \frac{(n_{i\alpha,j\beta\sigma})^2(n_{i\alpha',j\beta'\sigma'})^2}{W'_{\alpha\beta}} \right\}, \quad (95)$$

where $n_{i\alpha,j\beta\sigma}$ is an off-diagonal component of the density matrix, and $W'_{\alpha\beta}$ the mean energy of the virtual excitations associated with the $n_{i\alpha,j\beta\sigma}(\omega)$ density of states.

In order to understand the importance of the second term of Eq. (95), we consider first two different limiting cases. For a diatomic molecule, with a strong covalent bond (think of H_2), $(n_{11s,21s\sigma})^2 = n_{11s\sigma}(1-n_{11s\sigma}) = n_{21s\sigma}(1-n_{21s\sigma})$, and it is easy to see that the second term of Eq. (95) yields the same contribution as the first one. On the other limit, consider a crystal with an orbital per site having Z nearest neighbors. In this particular case (assuming the exchange hole located in the NN sites), we see that [Eqs. (12), (13)] $Z(n_{1,2\sigma})^2 = n_{1\sigma}(1-n_{1\sigma})$. Then we can conclude that the second term of Eq. (95) is Z times smaller than the first one. This simple argument shows why we can expect the second term of Eq. (95) to be important for molecules having localized bonds, and negligible for system having resonant bonds, such as Si. A detailed calculation of those terms confirms that the relative contribution of the off-diagonal diagram decays very quickly with the number of neighbors. Figures 14(a) and 14(b) show our results for HF and H_2O. In both cases, we calculate, using a minimal basis [HF: H(1s) and F($1s$,$2s$,$2p$), H_2O:H($1s$), and O($1s$,$2s$, and $2p$)], the first and second term of Eq. (95) as a function of the distance between atoms. Notice that in the case of H_2O, we keep the molecule angle constant, and change simultaneously both HO distances. These results show the importance of including the second term of Eq. (95) for the accurate determination of the correlation energy for small molecules. At the same time, they confirm that its relevance decays rapidly with the number of atoms in the molecule: the off-diagonal contribution of Eq. (95) is much more important for HF than for H_2O. F and O provide the larger contribution to the intraatomic correlation energy in these two molecules. The reduction in the contribution of the off-diagonal terms is related to the number of neighbors that each of these atoms has in the corresponding molecule: while F has only one neighboring H in HF, the oxygen has two H atoms as neighbors in H_2O.

In order to calculate the correlation energy $E^I[\{n_{i\alpha\sigma}\}]$ of the molecule to all orders in U_i, we have extended our approach of Sec. III, and introduced an interpolation between the $U_i \to \infty$ and the $U_i \to 0$ limits, taking into account that the dominant term contributing to $E^I[\{n_{i\alpha\sigma}\}]$ for molecules,the first term in the right-hand side of Eq. (75), can be approximated by a similar expression with $x_{i\alpha\sigma}$ redefined by the equation

$$x_{i\alpha\sigma} = \sum_{\beta\sigma'(\neq\alpha\sigma)} \frac{\tilde{U}_i}{W_{\alpha\beta}} n_{i\beta\sigma'}(1-n_{i\beta\sigma'}) + \sum_{j(\neq i),\alpha'\sigma'(\neq\alpha\sigma),\beta\sigma\neq\beta'\sigma'} \frac{\tilde{U}_j}{W'_{\alpha\beta}} \times \frac{(n_{i\alpha,j\beta\sigma})^2(n_{i\alpha',j\beta'\sigma'})^2}{n_{i\alpha\sigma}(1-n_{i\alpha\sigma})}, \quad (96)$$

where the second term represents the new off-diagonal term associated with the diagrams of Fig. 13. In practice, we calculate $E^I[\{n_{i\alpha\sigma}\}]$ defining a parameter $\eta_{i\alpha\sigma}$ such that

$$\eta_{i\alpha\sigma} = 1 + \frac{\sum_{j(\neq i),\alpha'\sigma'(\neq\alpha\sigma),\beta\sigma\neq\beta'\sigma'} (\tilde{U}_j/W'_{\alpha\beta})[(n_{i\alpha,j\beta\sigma})^2(n_{i\alpha',j\beta'\sigma'})^2/n_{i\alpha\sigma}(1-n_{i\alpha\sigma})]}{\sum_{\beta\sigma'\neq\alpha\sigma} (\tilde{U}_i/W_{\alpha\beta})n_{i\beta\sigma'}(1-n_{i\beta\sigma'})} \quad (97)$$

and replace, in Eq. (75), $x_{i\alpha\sigma}$ by $\eta_{i\alpha\sigma}x_{i\alpha\sigma}$.

Our proposal provides a very good description of the correlation energy. Figure 15 compares our estimate for $E^I[\{n_{i\alpha\sigma}\}]$ with the result of a standard configuration interaction (CI) calculation for the HF molecule. We have used in both calculations a minimal basis. The agreement between the two results is excellent, in despite of the quite different complexity of the two methods. This is specially important considering how the computational effort increases with the number of atoms in the molecule: the cost of our method increases linearly with the number of orbitals, in contrast with the factorial behavior of CI calculations. The same method can be applied to calculations with extended basis. Figures 16(a) and 16(b) compare the total energy for HF and H_2O calculated with a minimal basis (dashed line) and more complete basis (continuous line) [HF: H($1s$,$2s$,$2p$) and F($1s$,$2s$,$2p$, and $3d$), H_2O:H($1s$,$2s$,$2p$) and O($1s$,$2s$,$2p$, and $3d$)]. These results confirm the variational character of our approach. Finally, it has to be emphasized that our approach provides a significant improvement over other approximate methods commonly used in quantum chemistry as Moller-Plesset (MP) calculations.[44] MP calculations provide a good description of the correlation effects close to the energy minimum. Our approach reproduces well that distance

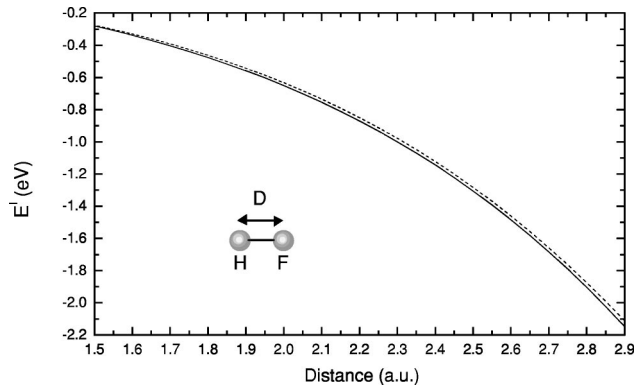

FIG. 15. Correlation energy for HF calculated using (a) a CI method (full line); (b) our approach (dashed line).

range (as shown in the examples above) and provides a very good description of the highly correlated limit relevant for large interatomic distances.

VI. CONCLUSIONS

The main body of this paper is addressed to analyzing generalized Hubbard Hamiltonians, showing how within a DMF approximation one can find either a local density or a many-body solution. In our LD approach, we show how to define an appropriate *local* potential associated with each of the localized orbitals used in the LCAO Hamiltonian. In our many-body solution, we introduce an appropriate self-energy for a degenerate multilevel case and calculate, using conventional Green-function techniques, the general electronic properties of the system.

We have applied these ideas to a multilevel Anderson model of an impurity, a quantum dot or a lattice, and have found that our results can be applied to an extensive range of parameters (typically, for $U/T \lesssim 10$) that covers most of the cases one is interested in.

In a second step, we have also considered how to use our previous analysis for studying more general cases, say, crystals or molecules. We have shown how one has to extend generalized Hubbard Hamiltonians to analyze these cases and have found, considering the crystal Si and the molecules HF and H_2O, good results for the ground state energies of these examples. This comfirms, not only the validity of our approach for generalized Hubbard Hamiltonians, but also, the validity of our extension to more realistic systems. In conclusion, we expect to have shown that the approach presented in this paper offers a very promising method for analyzing in a very realistic way the properties of highly correlated systems.

ACKNOWLEDGMENTS

P.P. and J.M.B gratefully acknowledge financial support by the Consejeria de Educacion y Cultura de la Comunidad de Madrid. This work has been supported by the CICyT (Spain) under Contracts No. PB97–0028 and No. PB97–0044.

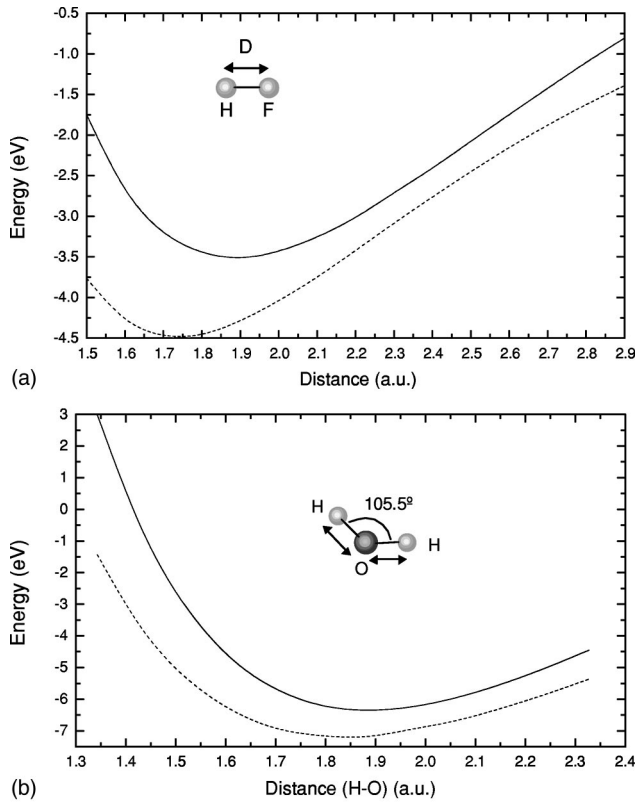

FIG. 16. (a) Binding energy for HF: full line, optimized minimal basis; dotted line: $H(1s,2s,2p)F(1s^2,2s^2,2p^2,3d)$. (b) Same for H_2O. The extended basis used in this case is the following: $H(1s,2s,2p)O(1s^2,2s^2,2p^2,3d)$. Experimental heats of formation (Ref. 45) for these molecules are: 6.120 eV (HF) and 10.167 eV (H_2O).

APPENDIX A: CALCULATION OF THE ATOMIC GREEN FUNCTION

The atomic Green function of Hamiltonian (30) is calculated using the conventional equation of motion:

$$\omega\langle\langle \hat{A};\hat{B}\rangle\rangle = \langle 0|\hat{A}\hat{B}+\hat{B}\hat{A}|0\rangle + \langle\langle [\hat{A},\hat{H}^{\mathrm{at}}];\hat{B}\rangle\rangle, \quad \text{(A1)}$$

where $\hat{A}$ and $\hat{B}$ are general fermion operators, $|0\rangle$ is the ground state of the atomic system, and $\langle\langle \hat{A};\hat{B}\rangle\rangle$ the Fourier-transformed in time of the retarded Green function $-i\theta(t-t')\langle 0|\hat{A}(t)\hat{B}(t')+\hat{B}(t')\hat{A}(t)|0\rangle$.

Starting with $\hat{A}=\hat{c}_{i\alpha\sigma}$ and $\hat{B}=\hat{c}^{\dagger}_{i\alpha\sigma}$, we obtain $G^{(at)\sigma}_{i,\alpha\alpha}$ as a function of new two-body Green functions

$$(\omega - E^{\sigma}_{i\alpha})G^{(at)\sigma}_{i\alpha\alpha} = 1 + \sum_{\beta\sigma'(\neq\alpha\sigma)} \tilde{U}_i \langle\langle \hat{c}_{i\alpha\sigma}\hat{n}_{i\beta\sigma'};\hat{c}^{\dagger}_{i\alpha\sigma}\rangle\rangle. \quad \text{(A2)}$$

New equations for each of these Green functions have to be obtained, in such a way that other new three-body Green functions appear. The procedure has to be repeated again and again until we get a system of closed equations. This can be finally achieved for the atomic Hamiltonian [Eq. (30)] due to the finite number of orbitals the atom has.

APPENDIX B: THREE-POLE APPROXIMATION FOR THE ATOMIC GREEN FUNCTION

The coefficients A_n^α of the Green function

$$G_{i,\alpha\alpha}^{(at)\sigma}=\frac{A_0^\alpha}{\omega-E_{i\alpha}^\sigma+i0^+}+\cdots+\frac{A_{N_i}^\alpha}{\omega-E_{i\alpha}^\sigma-\tilde{U}_iN_i+i0^+}+\cdots+\frac{A_{2M-1}^\alpha}{\omega-E_{i\alpha}^\sigma-\tilde{U}_i(2M-1)+i0^+} \tag{B1}$$

with A_n^α given by Eq. (31), can be found directly to satisfy the following sum rules:

$$\sum_{n=0}^{2M-1}A_n^\alpha=1, \tag{B2}$$

$$\sum_{n=0}^{2M-1}nA_n^\alpha=\sum_{\beta\sigma'\neq\alpha\sigma}\langle\hat{n}_{i\beta\sigma'}\rangle, \tag{B3}$$

$$\sum_{n=0}^{2M-1}n^2A_n^\alpha=\sum_{\beta\sigma'\neq\alpha\sigma}\langle\hat{n}_{i\beta\sigma'}\rangle+\sum_{(\beta\sigma')\neq\gamma\sigma'')\neq\alpha\sigma}\langle\hat{n}_{i\beta\sigma'}\hat{n}_{i\gamma\sigma''}\rangle \tag{B4}$$

with higher sum rules associated with correlation functions depending on more than two particles. Equations (33)–(35) are particular cases of Eqs. (B2)–(B4), for the Green function of Eq. (32).

APPENDIX C: GENERALIZATION OF EQ. (73)

Here, we discuss how to generalize Eq. (73) into the form (74), where new values $\langle a\rangle$, $\langle b\rangle$ and $\langle c[n_{i\alpha\sigma}(1-n_{i\alpha\sigma})/T^2]\rangle$, have been introduced.

Consider, as an example, the third case $\langle c[n_{i\alpha\sigma}(1-n_{i\alpha\sigma})/T^2]\rangle$. Values of c for different $\tilde{U}/T$ and M have been given in Table II. Assume that these values can be fitted by an interpolative equation that takes the form

$$c=\left[c_0+c_0'\frac{\tilde{U}}{T}+c_0''\left(\frac{\tilde{U}}{T}\right)^2\right]+\left[c_1+c_1'\frac{\tilde{U}}{T}+c_1''\left(\frac{\tilde{U}}{T}\right)^2\right]2M+\left[c_2+c_2'\frac{\tilde{U}}{T}+c_2''\left(\frac{\tilde{U}}{T}\right)^2\right](2M)^2 \tag{C1}$$

(more general polynomials can be easily used in the form explained below).

In the mean value $\langle c[n_{i\alpha\sigma}(1-n_{i\alpha\sigma})/T^2]\rangle$ we find different terms, behaving as

$$\tilde{c}_i\left(\frac{\tilde{U}}{T}\right)^r(2M)^s\frac{n_{i\alpha\sigma}(1-n_{i\alpha\sigma})}{T^2} \tag{C2}$$

where $\tilde{c}_i$ is a constant. Our way of defining $\langle c[n_{i\alpha\sigma}(1-n_{i\alpha\sigma})/T^2\rangle$ implies replacing terms such as (C2), by the equation

$$\tilde{c}_i\tilde{U}^r\frac{\left[\sum_{\alpha\sigma}n_{i\alpha\sigma}^{3/s+1}(1-n_{i\alpha\sigma})^{3/s+1}\right]^{s+1}}{\sum_{\alpha\sigma}T_\alpha^{r+2}n_{i\alpha\sigma}^2(1-n_{i\alpha\sigma})^2}. \tag{C3}$$

Notice that for $n_{i\alpha\sigma}=n_i$ and $T_\alpha=T$, Eq. (C3) goes into (C2), since the term multiplying $\tilde{c}_i\tilde{U}^r$ in Eq. (C3) behaves as $(2M)^s$ and the other factors are immediately recovered.

Equation (C3) is introduced taking as the weighting factor of each orbital $n_{i\alpha\sigma}^2(1-n_{i\alpha\sigma})^2$, and adjusting the T power and the $n_{i\alpha\sigma}(1-n_{i\alpha\sigma})$ power of the numerator to the limit given by Eq. (C2). Another example, coming from the average of a, would be the term

$$\tilde{a}_i\left(\frac{\tilde{U}}{T}\right)^r(2M)^s, \tag{C4}$$

with $\tilde{a}_i$ also being a constant. In this case, we replace Eq. (C4) by

$$\tilde{a}_i\tilde{U}^r\frac{\left[\sum_{\alpha\sigma}n_{i\alpha\sigma}^{2/s+1}(1-n_{i\alpha\sigma})^{2/s+1}\right]^{s+1}}{\sum_{\alpha\sigma}T_\alpha^rn_{i\alpha\sigma}^2(1-n_{i\alpha\sigma})^2}. \tag{C5}$$

[1] P. Hohenberg and W. Kohn, Phys. Rev. **136**, 864 (1964).

[2] R.M. Dreizler and E.K.U. Gross, *Density Functional Theory* (Springer-Verlag, Berlin, 1990).

[3] *The Single-Particle Density in Physics and Chemistry*, edited by N.H. March and B.M. Deb (Academic, London, 1987).

[4] W. Kohn and L.J. Sham, Phys. Rev. **140**, A1133 (1965).

[5] R.O. Jones and O. Gunnarson, Rev. Mod. Phys. **61**, 689 (1989).

[6] J.P. Perdew, J.A. Chevary, S.H. Vosko, K.A. Jackson, M.R. Pederson, D.J. Singh, and C. Fiolhais, Phys. Rev. B **46**, 6671 (1992); J.P. Perdew, K. Burke, and M. Ernzerhof, Phys. Rev. Lett. **77**, 3865 (1996).

[7] L. Hedin and S. Lundqvist, in *Solid State Physics*, edited by H. Ehrenreich, F. Seitz, and D. Turnbull (Academic, New York, 1969), Vol. 23; J. Callaway and N.H. March, *ibid.* (Academic, New York, 1984), Vol. 38.

[8] L. Hedin, in *Elementary Excitations in Solids, Molecules and Atoms*, edited by J.T. Devreese, A.B. Kunz, and T.C. Collins (Plenum, New York, 1974).

[9] M.S. Hybertsen and S.G. Louie, Phys. Rev. Lett. **55**, 1418 (1985).

[10] R. Godby, M. Schluter, and L.J. Sham, Phys. Rev. Lett. **56**, 2415 (1986).

[11] V.I. Anisimov, I.V. Solovyev, M.A. Korotin, M.T. Czyzyk, and G.A. Sawatsky, Phys. Rev. B **48**, 16 929 (1993); M.T. Czyzyk and G.A. Zawatzky, *ibid.* **49**, 14 211 (1994).

[12] J. Ihm, A. Zunger, and M.L. Cohen, J. Phys. C **12**, 4409 (1979); M.C. Payne, M.P. Teter, D.C. Allan, T.A. Arias, and J.D. Joannopoulos, Rev. Mod. Phys. **64**, 1045 (1992).
[13] O.F. Sankey and D.J. Niklewski, Phys. Rev. B **40**, 3979 (1989).
[14] B. Delley, J. Chem. Phys. **92**, 508 (1990).
[15] G. te Velde and E.J. Baerends, Phys. Rev. B **44**, 7888 (1991).
[16] Z. Lin and J. Harris, J. Phys.: Condens. Matter **5**, 1055 (1993).
[17] A.A. Demkov, J. Ortega, O.F. Sankey, and M.P. Grumbach, Phys. Rev. B **52**, 1618 (1995).
[18] T. Zhu, W. Pan, and W. Yang, Phys. Rev. B **53**, 12 713 (1996).
[19] J. Hartford, L.B. Hansen, and B.I. Lundqvist, J. Phys.: Condens. Matter **8**, 7379 (1996).
[20] D. Sanchez-Portal, P. Ordejon, E. Artacho, and J.M. Soler, Int. J. Quantum Chem. **65**, 453 (1997).
[21] A.P. Horsefield, Phys. Rev. B **56**, 6594 (1997).
[22] P. Pou, R. Pérez, J. Ortega, and F. Flores, in *Tight-Binding Approach to Computational Materials Science*, edited by P.E.A. Turchi, A. Gonis, and L. Colombo, MRS Symp. Proc. No. 491 (Materials Research Society, Pittsburgh, 1998), p. 45.
[23] See, for example, Comput Mater. Sci. **12**, 157 (1998).
[24] A. Georges, G. Kotliar, W. Krauth, and M.J. Rozenberg, Rev. Mod. Phys. **68**, 13 (1996).
[25] F. Flores, J. Ortega, and R. Pérez, Surf. Rev. Lett. **6**, 411 (1999).
[26] F.J. García-Vidal, J. Merino, R. Pérez, R. Rincón, J. Ortega, and F. Flores, Phys. Rev. B **50**, 10 537 (1994).
[27] E. Müller-Hartmann, Int. J. Mod. Phys. B **3**, 2169 (1989); W. Hetzner and D. Vollhardt, Phys. Rev. Lett. **62**, 324 (1989).
[28] A. Levy-Yeyati, F. Flores, and A. Martin-Rodero, Phys. Rev. Lett. **83**, 600 (1999).
[29] A. Martin-Rodero, F. Flores, M. Baldo, and R. Pucci, Solid State Commun. **44**, 911 (1982).
[30] H. Kajueter and G. Kotliar, Phys. Rev. Lett. **77**, 131 (1996); M. Potthoff, T. Wegner, and W. Nolting, Phys. Rev. B **55**, 16 132 (1997).
[31] A.I. Lichtenstein and M.I. Katsnelson, Phys. Rev. B **67**, 6884 (1998).
[32] A. C. Hewson, *The Kondo Problem to Heavy Fermions* (Cambridge University Press, Cambridge, 1993); D.C. Langreth, Phys. Rev. **150**, 516 (1966).
[33] J.M. Luttinger and J.C. Ward, Phys. Rev. **118**, 1417 (1960).
[34] J.P. Perdew, R.G. Parr, M. Levy, and J.L. Balduz, Phys. Rev. Lett. **49**, 1691 (1982).
[35] D. Spanjard and M.C. Desjonqueres, in *Interaction of Atoms and Molecules with Solid Surfaces*, edited by E. Bortolani *et al.* (Plenum, New York, 1990).
[36] S. Horshfield, J.H. Davies, and J.W. Wilkins, Phys. Rev. Lett. **67**, 3720 (1991).
[37] Y. Meir, N.S. Wingreen, and P.A. Lee, Phys. Rev. Lett. **70**, 2601 (1993).
[38] T.K. Ng and P.A. Lee, Phys. Rev. Lett. **61**, 1768 (1988).
[39] A. Levy-Yeyati, A. Martín-Rodero, and F. Flores, Phys. Rev. Lett. **71**, 2991 (1993).
[40] T. Homoi and K. Kubo, Phys. Rev. B **58**, R567 (1998).
[41] N.E. Bickers, Rev. Mod. Phys. **59**, 845 (1984).
[42] W.R.L. Lambrecht and O.K. Andersen, Phys. Rev. B **34**, 2439 (1986).
[43] F. Flores, A. Levy-Yeyati, A. Martin-Rodero, and J. Merino, Phys. Low-Dimens. Semicond. Struct. **1**, 23 (1994).
[44] See, E. Clementi, in *Modern Techniques in Computational Chemistry: MOTECC-89* (ESCOM, Leiden, 1989), p. 324.
[45] See, E. Clementi, in *Modern Techniques in Computational Chemistry: MOTECC-89* (ESCOM, Leiden, 1989), p. 608.